

PRELIMINARY INVESTIGATION OF A FLAX-EPOXY COMPOSITE MATERIAL FOR
ORTHOPAEDIC APPLICATIONS

By

Kamil Shami

BEng. in Mechanical Engineering
Ryerson University, Toronto, 2009

A thesis

presented to Ryerson University

In partial fulfillment of the
requirements for the degree of

MASTER OF APPLIED SCIENCE

In the Program of
Mechanical Engineering

Toronto, Ontario, Canada, 2012

© Kamil Shami, 2012

Author's Declaration

I hereby declare that I am the sole author of this thesis. This is a true copy of the thesis, including any required final revisions, as accepted by my examiners.

I authorize Ryerson University to lend this thesis to other institutions or individuals for the purpose of scholarly research

I further authorize Ryerson University to reproduce this thesis by photocopying or by other means, in total or in part, at the request of other institutions or individuals for the purpose of scholarly research.

I understand that my thesis may be made electronically available to the public

Abstract

Preliminary Investigation of a Flax-Epoxy Composite Material for Orthopaedic Applications

Master of Applied Science, 2012

Kamil Shami

Mechanical Engineering

Ryerson University

In this dissertation, a preliminary experimental study was done on a flax-epoxy prepreg to determine its suitability as a composite material for making bone fixation plates. The research involved manufacturing, testing, data analysis, and design and optimizing. The material was found to have sufficient strength and mechanical characteristics similar to those of bone, and could be used for making bone fixation implants with proper design or in combination with other reinforcement fibres. The findings of this research are useful not only for using flax-epoxy composites in designing bone fixation plates but also for orthopaedic implants, such as joint replacement, in general.

Acknowledgment

The author of this dissertation would like to thank Dr. Habiba Bougherara and Dr. Zouher Fawaz for their efforts in supporting and facilitating the completion of this research work

The author would also like to thank Dr. Ihab El-Sawi and PHD candidate Mr. Giovanni Montesano for their valuable help with the experimental work

Table of Contents

Abstract	iii
Acknowledgment	iv
List of Tables	vii
List of Figures	viii
Nomenclature	xi
1. Introduction.....	1
1.1 Composite Materials	1
1.2 Natural Composites	1
1.3 Composites as Orthopaedic Implants.....	2
2. Research Objective	3
3. Literature Review.....	4
3.1 Flax Fibres.....	4
3.2 Flax Fibres Composites	6
3.3 Fibre Composites as Orthopaedic Implants	9
3.4 Challenges in Designing Bone Plates.....	11
4. Methodology	14
4.1 Manufacturing	14
4.2 Testing.....	14
4.3 Implant Design and Optimization	15
5. Manufacturing.....	16
5.1 Layout.....	16
5.2 Curing.....	16
6. Testing.....	18
6.1 Tensile Test	18
6.2 Bending Test	19
6.3 Fatigue Test	20
7. Results.....	21
7.1 Tensile Test Results	21

7.2 Bending Test Results.....	40
7.3 Fatigue Test Results	52
8. Discussion.....	53
8.1 Longitudinal Properties of Unidirectional Samples.....	53
8.2 Transverse Properties of Unidirectional samples.....	54
8.3 Longitudinal Properties of Two-Directional Samples	54
8.4 Flexural Properties of Unidirectional Samples	55
8.5 Flexural Properties of Two-Directional Samples.....	56
8.6 Flax-Epoxy Composites for Bone Fixation Plates	56
8.7 Optimization of Plate Design	58
9. Conclusions.....	61
10. References.....	64
11. Appendix A.....	69
12. Appendix B	71

List of Tables

Table 1: Longitudinal tensile test results of unidirectional samples	21
Table 2: Transverse tensile test results of unidirectional samples	24
Table 3: Poisson's ratio at different curing temperatures	24
Table 4: Shear modulus	24
Table 5: Tensile test results of unidirectional and two-directional samples	27
Table 6: Tensile test results of design samples	28
Table 7: Bending test results for unidirectional samples	40
Table 8: Regional and average flexural modulus values for unidirectional samples	40
Table 9 : Bending test results for design samples	41
Table 10: Flexural modulus values for design samples	41
Table 11: Fatigue test results of design samples	52
Table 12: Summary of optimized design parameters	59

List of Figures

Figure 1: Mapping and cutting of prepreg composite layers	16
Figure 2: Composite role with layers cut out.....	16
Figure 3: Composite layers before lay-up.....	17
Figure 4: Lay-out of composite layers	17
Figure 5: Preparation of the mould	17
Figure 6: Composite plate inside the mould	17
Figure 7: Pressure system inside the oven	17
Figure 8: UNITED tensile test machine.....	18
Figure 9: A view of the grips used for tensile testing	18
Figure 10: Tensile test with extensometer - close view	19
Figure 11: Tensile testing with extensometer	19
Figure 12: Bending test - close view.....	19
Figure 13: Bending test.....	19
Figure 14: Bending test - near the end of test side view	20
Figure 15: Bending test - near the end of test	20
Figure 16: Fatigue testing	20
Figure 17: Fatigue testing - close view	20
Figure 18: Ultimate strength of unidirectional samples.....	22
Figure 19: Maximum strain of unidirectional samples	23
Figure 20: Young's modulus values of unidirectional samples	23
Figure 21: Transverse strength of unidirectional samples	25
Figure 22: Maximum transverse strain of unidirectional samples.....	26
Figure 23: Transverse Young's modulus of unidirectional samples	26
Figure 24: Ultimate tensile strength of composites with different ply orientation	29
Figure 25: Maximum strain of composites with different orientation.....	30
Figure 26: Young's modulus of composites with different ply orientation	30
Figure 27: Tensile strength of design samples.....	31
Figure 28: Maximum strain of design samples.....	32

Figure 29: Young's modulus of design samples	32
Figure 30: Tensile behaviour of unidirectional sample T4 cured at 110 °C.....	33
Figure 31: Young's Modulus of unidirectional sample T4 cured at 110 °C	34
Figure 32: Tensile behaviour of unidirectional sample T17 cured at 150 °C.....	34
Figure 33: Young's modulus of unidirectional sample T17 cured at 150 °C.....	35
Figure 34: Tensile behaviour of design sample T13 cured at 110 °C.....	35
Figure 35: Young's modulus of design sample T13 cured at 110 °C	36
Figure 36: Transverse behaviour of unidirectional sample T22 cured at 110 °C	37
Figure 37: Transverse modulus of unidirectional sample T22 cured at 110 °C	38
Figure 38: Transverse behaviour of unidirectional sample T18 cured at 150 °C	38
Figure 39: Transverse modulus of unidirectional sample T18 cured at 150 °C	39
Figure 40: Bending failure loads of unidirectional samples	42
Figure 41: Ultimate flexural strength of unidirectional samples	43
Figure 42: Maximum deflection of unidirectional samples	43
Figure 43: Maximum outer-surface strain of unidirectional samples	44
Figure 44: Flexural modulus of unidirectional sample	44
Figure 45: Bending failure loads of design samples	45
Figure 46: Ultimate flexural strength of design samples	46
Figure 47: Maximum deflection of design samples.....	46
Figure 48: Maximum outer-surface strain of design samples.....	47
Figure 49: Flexural modulus of design sampl.....	47
Figure 50: Flexural behaviour of unidirectional sample B5 cured at 110 °C	48
Figure 51: Regions of flexural behaviour of unidirectional sample B5 cured at 110 °C	49
Figure 52: Flexural behaviour of unidirectional sample B10 cured at 150 °C	49
Figure 53: Regions of flexural behaviour of unidirectional sample B10 cured at 150 °C	50
Figure 54: Flexural behaviour of design sample B1 cured at 110 °C.....	50
Figure 55: Regions of flexural behaviour of design sample B1 cured at 110 °C	51
Figure 56: Comparison of Young's modulus values of different materials	60
Figure 57: Failure of samples under tensile load - vertical view	69

Figure 58: Failure of samples under tensile load - horizontal view.....	69
Figure 59: Simple outer-surface failure under flexural load.....	69
Figure 60: Simple outer-surface failure under flexural load - close view	69
Figure 61: Combined outer-surface tensional failure and inner-surface compressive failure under flexural load	70
Figure 62: Complex outer-surface tensional failure, inner-surface compressive failure, and delamination under flexural load	70

Nomenclature

σ : Stress

ϵ : Strain

E: Young's Modulus

P: Load

A: Cross sectional area

b: Width

h: Height

L: Length

1. Introduction

1.1 Composite Materials

Composite materials have replaced metallic materials in various engineering applications in a number of industries including transportation, aerospace, pressure vessel and others. Some of the advantages of composite materials are their lightweight, low density and high strength to weight ratio. Most importantly, what makes composite materials superior to other types of materials is their flexibility to be manipulated to achieve certain desired properties that cannot otherwise be achieved by the elementary constituent materials on their own. The properties of composite materials are determined by the properties, ratios, and orientation of their constituent parts. A composite material typically consists of a bonding material called the matrix, and one or more reinforcing materials called the fibres. Examples of common matrices are thermoplastics (polypropylene, polyester) and thermosetting (phenolics, epoxies), while examples of common reinforcement include glass fibres and carbon fibres.

1.2 Natural Composites

One drawback of composite materials is that they can be more costly than the materials they are replacing, often because of the high cost of the fibres. Environmentally, composite materials made with synthetic fibres (glass, carbon etc.) cannot be recycled and have to be disposed with. Research into reducing the costs associated with composite materials while making them environmentally friendly has led to the idea of using natural fibres, taken from plants, as the reinforcing material. Natural fibres are cheap, widely available and come from renewable source. They include: jute, flax, hemp, ramie, kenaf, sisal, palf, henequen, cotton, coir, wood and others. Flax fibres in particular were found to have superior qualities suitable for composites and have been studied both separately and as composites with various types of thermoplastic and thermosetting matrices. One type of flax fibre composites that has been recently developed is the flax-epoxy prepreg in which flax fibres are pre-impregnated with epoxy and delivered to the user in a frozen state.

1.3 Composites as Orthopaedic Implants

One area where there has been growing interest in the use of composite materials is medical implants. Traditionally, metals have been used as implants to fix fractured bones or as orthopaedic replacement of joints. Metals have the drawbacks of being susceptible to corrosion in biological environments as well as being heavy and having much higher stiffness than human bones. The use of metallic implants as bone fixation plates affects the healing process of the fractured bone since the implant, having a much higher stiffness than the bone, ends up carrying most of the body weight of the patient. This prevents sufficient formation of the callus since the bone does need to experience stresses and strains as stimulus to growth and self-reparation. Research has been done on the use of various non-metallic composites to replace metals in medical implant applications. Examples of that include carbon-carbon composites, glass-polymer composites, carbon-polymer composites and others. However, very little research has been done on the use of natural fibre composites, especially flax composites, which are thought to have mechanical properties similar to those of long cortical bones.

2. Research Objective

The purpose of this study is to determine the suitability of flax-epoxy prepreg composites for making bone fixation plates. Samples of the flax-epoxy prepreg composite material will be subjected to a variety of mechanical tests including tension, flexural and fatigue in order to mechanically characterize the material and try to reach the most suitable design (number of layers, thickness, orientation etc) for the composite to be used as a bone fixation implant. The results can also be useful for applications other than those intended as the direct purpose of this research such as the use of flax-epoxy composites for making joint replacements or even parts for the aerospace or transportation industries.

3. Literature Review

3.1 Flax Fibres

Flax is probably the oldest easily cultivated fabric fibre known to mankind. It has been used for centuries in fabrication of fine linens, ropes, mats and carpets [1]. In Modern times, Flax has been the source of many products in the textile, paper, and oil industries [2]. Additionally, flax straw has been used in the building industry as solidifying material, building board, and insulating and non-inflammable material [1]. The widespread use of flax can be attributed to its easy production and outstanding mechanical performance [3].

A number of reports show that a lot of research has been done on flax fibres; however, interest in using flax fibres as reinforcement in plastic matrix composites has risen only in the last few decades because of their low cost, low density, high specific strength and specific modulus, low corrosiveness, and widespread availability and renewability in nature in many countries around the globe [1]. However, because of uncertainties and difficulties in predicting their vastly variable and scattered properties and the influence of that on their derived polymeric composites, flax fibres are often used in low grade applications only [4, 5]. For example, the use of flax composites in the automotive industry has increased to a great extent recently as non-woven fibre mats in interior panels [6]. Pre-processed flax fibres, fibres mats, and continuous textile reinforcement have been used to produce oriented, quasi-unidirectional flax-polymer composites [7].

Flax has been found to possess the highest tensile strength among natural fibres. Mohanty et al. provided the following average numbers for flax fibre mechanical properties: tensile strength of 345-1100 MPa, Young's modulus of 27.6 GPa, and elongation to break of 2.7-3.2% [8]. Other researchers have reported different numbers, for example, Baley and Lamy in one of their papers gave an average Young's Modulus value of 54 GPa [9], and in another paper they gave a range of 30-110 GPa [10]. Charlet et al. from their literature review reported a tensile strength of 600 - 2000 MPa, Young's modulus of 12-100 GPa and ultimate tensile strain of 2% [5]. Aslan et al., by looking at previous research as well as from their own investigation, reported the following

ranges: tensile strength from 621 to 1834 MPa, Young's Modulus from 24 to 76 GPa, and strain to failure from 1.3 to 3.3% [4].

Such large variations in mechanical properties arrived at by different researchers can be attributed to the source of the fibres, their treatment and method of testing. Research has uncovered that the properties of flax fibres such as density, tensile strength, and Young's modulus depend on their internal structure and chemical composition which is in turn related to the size the maturity of fibres as well as the method adopted for their extraction [11]. Flax fibres are made of micro fibrils which in turn are made of cellulose cells, and since each type of cellulose has its own cell geometry and properties, different types of flax coming from different fields can vary greatly in their properties [1]. Flax fibres show variability in their cell wall structure depending on growth conditions, level of maturity and the effects of the retting and decortication processes used to extract them from their plants [4]. In addition, flax fibres are very delicate and have a variable polygonal cross section in the order of micrometers and a length of few millimetres making them difficult to measure and adding to the difficulty in characterizing them [4].

Non-uniform geometric characteristics is a general feature of natural fibres. Flax fibres have a polygonal shape with 5 to 7 sides and a non-constant transverse diameter where the fibres are thicker near the root and thinner near the tip [12]. According to Baley the width of flax fibres lie in the range of 5 to 76 μm and the length in the range of 4 to 77 mm. The flax fibre is made of highly crystalline cellulose fibrils spirally wound in a matrix of amorphous hemicelluloses and lignin, and the fibrils have a title angel of 10-11 degrees with respect to the longitudinal axis of the fibres hence displaying a unidirectional structure [12]. Flax fibres are arranged in small bundles made of several elementary flax fibres, called technical fibres, glued together by pectic cement [5]. Rowell et al. reported that elementary flax fibres can be extracted from technical fibre bundles and range in length from 5 to 88 mm and in diameter from 10 to 40 μm [13].

The cell walls of flax fibres contain numerous defects known as kink bands which can be observed with a scanning electronic microscope (SEM) or optical microscopy with a polarized light [12]. These defects are a result of natural growth of the cells of flax fibres and the change of their crystalline orientation, or can be the product of the process of decortication in which the

fibres are separated from the plants [12]. In flax fibre composites kink bands are highly undesirable since it is believed that stress concentration around these defects can act as the initiator of fibre-matrix debonding as well as the formation of micro-cracks in the matrix [14].

3.2 Flax Fibres Composites

Most biocomposites (natural fibre composites) consist of a polymer as the matrix and a natural fibre as the reinforcement and can be divided into two main categories: thermoplastic and thermosetting composites [1]. Thermosetting polymers have mechanical qualities far superior to thermoplastic polymers thus most researchers prepare flax composites using thermosetting resins as the matrix [15]. The mechanical properties of natural fibre composites depend on a number of parameters including fibre strength, length and orientation and the strength of the interfacial fibre-matrix bond. Some researchers have found that modifications, treatment, and processing of fibres as well as the addition of small amounts of chemicals such as dicumyl peroxide or benzoyl peroxide improve resistance to moisture degradation of the interfacial matrix bond and significantly improve the mechanical properties of the composite [16]. Others such as Stuart et al. in their study of the mechanical properties of treated and untreated flax reinforced epoxy composites found that the use of enzyme chelators to be a good environmentally friendly way of improving the quality of flax fibres for composite applications [17].

The tensile strength of flax reinforced composites is determined by the tensile strength of the fibres and to a great extent to the presence of defects and weak lateral fibre bonds [1]. Anderson and Joffe studied the effect of discontinuity, misalignment, and disorder in the fibre spacing in the matrix, due to the presence of fibre bundles, on the strength of flax fibre-polymer composites [7]. They produced a theoretical model of a polymer reinforced by perfectly aligned, continuous, and regularly spaced flax fibres and compared their results to experimental results from currently available flax-polymer composites. It was found that the current composites are 30% lower in tensile strength and stiffness from what is theoretically achievable through better processing and separation of flax fibre bundles into elementary fibres [7]. Similarly, Charlet et al. concluded from their study that the fact that fibres exist in the shape of small bundles in their derived composites may be responsible for low composite mechanical properties compared with those expected from the elementary flax fibres [5].

Baley et al. have studied the longitudinal and transverse tensile behaviour of unidirectional flax composites and found that the failure mode is very complex: cracks appear not only in the matrix and the fibre-matrix interface but also within the fibres and fibre bundles themselves [18]. They reported an average longitudinal Young's Modulus of 59 GPa and a Transverse Modulus of 8 GPa [18]. In another study, Baley and Lamy reported a longitudinal modulus of elasticity for unidirectional flax-epoxy composites that ranged from 18 GPa to 30 GPa based on a fibre volume fraction ranging from 30% to 50% [10]. Similarly, Charlet et al. in their survey of literature reported that the properties of unidirectional flax composites were 200 MPa for strength and 20 GPa for Young's Modulus at a fibre volume fraction of 40% [5].

Van Raemdonck et al. performed three-point flexural bending tests on unidirectional flax-epoxy prepregs and reported the flexural modulus of elasticity to range from 5 and 10 GPa and flexural strength from 110 to 170 MPa [19]. They also tested the effect of having an extra carbon layer on the outsides of the flax composite and found that the modulus of elasticity is almost tripled and the bending strength is more than doubled. However, their results had high variations which the author contributed to insufficient adhesion of the carbon fibres to the core flax material [19].

Aslan et al. found that flax fibres have both linear and non-linear stress-strain behaviour with the linear behaviour giving a higher tensile strength and Young's modulus, and a lower strain to failure than the non-linear behaviour [4]. They suggested that the two types were correlated with defects resultant from processing where the lowly processed fibres revealed only the linear behaviour while the highly processed fibres showed both linear and non-linear behaviours [4]. The same study concluded that fibres had a complex micro-scale fracture mechanism with large fracture zones governed by surface and internal defects causing crack propagation in both the longitudinal and transverse directions [4].

Charlet et al. reported that when a flax fibre is tensile loaded up to failure, the stress-strain curve shows a non-linear domain from a strain of about 0.3% until about 1.5% before becoming linear again [5]. The same study showed that when testing these fibres in their derived polymer composites, the shape of the stress-strain curves looked like those of the elementary flax fibres meaning that the adhesion between the fibres and the matrix is of a good quality, and that the fibres deform within their composites in the same way they do individually although they are in

the form of bundles rather than elementary fibres [5]. They also found that the reinforcement efficiency of flax fibres just before the composite failure did not exceed 30% meaning that only one third of initially embedded fibres were actually bearing the load just before fracture. This may be explained by the development of sliding within the fibre bundles throughout the test period and also the thermal damage undergone by the fibres during processing [5].

Romhany et al. observed the failure sequence of flax fibres, using SEM, to follow these superimposed steps: longitudinal splitting along the boundaries of fibres, transverse cracking of the fibres, and lastly fracture of fibres and their micro-fibrils [3]. Van Raemdonck et al. in their study of flax-epoxy prepregs observed from SEM images that resin residue can be seen on the fracture surface which suggests that the fibres were torn apart before the resin had released the fibres indicating good adhesion between the flax fibres and epoxy resin [19].

Moisture absorption is yet another issue that can greatly affect the overall performance of flax composites. Moisture sorption can influence the dimensional stability of flax composites and lead to decomposition and forming of micro-cracks in addition to fungal degradation if the moisture content is sufficiently high [19]. Chemical treatment of fibres can reduce moisture absorption by altering the surface chemistry of the fibres [2, 6]. Also, stronger intermolecular fibre matrix bonding through the use of additives as well the application of insulating coating to the composite can significantly improve moisture resistance of the flax fibres [1].

Van Raemdonk et al. used Dynamic Vapour Sorption (DVS) analysis to study the extent of moisture absorption in samples of hackled long flax, untreated flax fabric, and both uncured and cured flax-epoxy prepregs. They found that untreated flax fabric had lower moisture uptake than loose hackled long flax while prepreg fabric had lower moisture uptake than both and reported the following numbers for percentage changes in the mass of fibres (from initial dry mass): loose long hackled flax 15%, untreated flax fabric 12%, uncured flax-epoxy prepreg 4%, and cured flax-epoxy prepreg 2% [19]. European standards specify that a moisture uptake of 10% is the critical limit for applications under wet and humid conditions [19].

Van Raemdonk et al. also performed Basidiomycete testing to evaluate the resistance of flax fibres to white and brown rot (biological fungal degradation). They found that the mass loss of

the treated fabric composite based on a prepreg material did not exceed 3% when decayed by either brown or white rot fungus while the composites made of untreated flax fibres showed a mean mass loss of up to 35% [19]. Based on European standards, a critical value of 3% mass loss due to biological degradation indicates the acceptable fungal resistance of a material under humid and wet conditions [19].

One of the most successful flax composite technologies has been the flax-epoxy prepregs developed by a European company called Lineo. In an article in the JEC composite magazine in December 2007 named "Flax-Epoxy Prepregs Leading the race" the author listed the advantages of flax fibre composites and prepreg composites in particular. The properties of flax fibres are similar to those of standard glass fibre, however, flax fibres have a lower density than glass fibres and even carbon fibres with the added advantage of having vibration absorption qualities just like natural fibres in general [20]. Similarities between flax and carbon fibres such as having almost a zero coefficient of expansion and a break elongation of about 1.5% is an added value which allows for the making of high-performance flax-carbon hybrid composites [20]. The two most significant problems of flax composites are the poor adhesion between flax fibres and the resin and the tendency of flax fibres to absorb moisture. The use of the prepreg technology helps overcome these obstacles by creating strong fibre-matrix bonds and limiting the water uptake of flax fibres to only 2% which is similar to what is found in glass and carbon composites [20].

3.3 Fibre Composites as Orthopaedic Implants

In bone surgery, metallic implants are usually used to fix fractures due to their high strength, toughness and easy machining. However, metal implants have two important drawbacks: susceptibility to corrosion in biological mediums, and over-stiffening due to the large difference between the Young's modulus of metals and that of bones [21, 22]. Therefore, search for alternative materials has occupied the minds of many researchers. Fibre reinforced composites have been studied as a substitute to metallic implants because of their microstructural similarity to bone tissue and flexibility of their mechanical properties [23, 24]. The use of composites as implants in medical application is conditioned by the biofuncionality and biocompatibility of both the fibre and matrix where biofuncionality means that the mechanical properties of the material should as closely as possible match those of the bone tissue and biocompatibility means

that the chemical properties of the composites should be compatible with those of the natural tissue [25].

It is very important for biofunctionality that the composite material is capable of producing implants with high strength, high fracture energy and low Young's modulus close to that of the bone tissue which is about 20 GPa. Chlopek and Kmita pointed out that this can be achieved by having composites with two dimensional, three dimensional or even multi-dimensional fibre orientation. They gave carbon composites as an example of this where a unidirectional carbon composite has a Young's modulus of 50-300 GPa, two-dimensional of 20-30 GPa, three-dimensional of 10-20 GPa, and multidimensional of 1-10 GPa [25]. Also, the arrangement of the fibres affects the porosity of the matrix (pore size and distribution) which is decisive for biocompatibility given by both biological reaction and fixation to the bone tissues [25].

The selection of an appropriate matrix material is particularly important since its properties affect not only the mechanical properties of the composite but also its biological ones such the capability of fixation to the bone tissue; however, the great difficulty in obtaining biocompatible composites remains finding biocompatible fibres [25]. Different references suggest a variety of biocompatible materials that can serve the role of the matrix: HAP (Hydroxyapatite), TCP (Tricalcium Phosphate), bioglasses, inert ceramics, inert and resorbable polymers (PSU, PLA, GLA, PEEK, Epoxy) and carbon materials while biofunctional reinforcing fibres include: HAP, Alumina, bioglasses, carbon, and polylactide [26-31].

Chlopek and Kmita observed two mechanisms of fixation between Carbon-Carbon composite implants and the bone which depends on the porosity of the composite material. In unidirectional composites, which have small pores, mechanical bonding happens only at the surface as it is the case with metallic implants. However, in three-dimensional composites, the composite pores are larger (mean pore diameter is 100 μm) and create an open system of channels near the surface of the implant which allows for bone tissue growth into the implant [25]. This type of bonding is much stable than sole surface bonding since the composite implant can undergo gradual degradation under biological conditions [25].

Implants can also be made of polymer composites. Research by Chlopel et al. on developing polymer implants for hip joint replacement found that the best results were obtained when using carbon-epoxy composites [32]. These composites were found to be perfectly biomechanically compatible with the bone tissue, but at the same time inferior to Carbon-Carbon composites due to their low porosity which did not allow for the formation of biological ingrowth bonds [25]. Chlopek et al. as well as Stoch et al. suggest that in such a case, the bonding strength can be increased by coating the composite material by layers of a bioactive material [33, 34].

Some researchers have looked into employing natural fibre composites as bone implants and fixation plates. Chandramohan and Marimuthu have done extensive work on designing and testing sisal, banana, and roselle polymer composites for bone replacements or bone fixing plates [35, 36]. They applied a variety of tests including moisture absorption, flexural, tensile and impact tests on their samples and observed, using SEM, that the forms of failure of these composite varied based on the type of fibre or hybrid of fibres used for reinforcement where some composites were more brittle while some experienced more fibre pull-out than others [36]. Composites which exhibited more fibre pull-out were found to be superior at withstanding impact [36]. They also found that the presence of moisture in the composites weakens the fibre-matrix interface, leads to poor stress transfer, and reduces the flexural strength. [35]. To remedy this problem, they recommended the use of calcium phosphate and hydroxy apatite as external coating [35, 36]. They concluded that by comparison to stainless steel, cobalt chrome, titanium, and zirconium implants, sisal, banana, and roselle composites were suitable as promising implant materials for both internal and external fixation of fractured bones [35, 36].

3.4 Challenges in Designing Bone Plates

Bone plates are used to hold fractured bone segments firmly in position thus providing immobilization at the fracture site and allowing primary bone healing and endosteal callus formation [37]. Plates made of stainless steel, titanium, and cobalt-chromium alloys are suitable for this purpose. However, studies have shown that the high Young's modulus of metal plates results in the majority of the load being born by the metallic plate while very little is taken by the bone itself which is known as stress shielding [37]. Experimental studies such as the one done by Tonino et al. showed that the lack of stress in the bone leads to the prevention of callus

formation, ossification and bone union which causes both the fractured part and the whole bone to become osteoporosis [38]. Tayton and Bradley found that the design and material of bone plates should allow for at least 2% compressive strain at the fracture site to improve callus formation at the initial stage of healing [39]. These recommendations are echoed by Perren who found in his study that appropriate mechanical stimulus such as relative micro-movement at the fracture site stimulated generation of callus tissues and that interfragmentary strains (strains at the fracture) ranging from 2% to 10% were the most appropriate condition for healing bone fractures [40].

Claes conducted an experimental study in which he compared two plates of different stiffness values but similar dimensions: a stainless steel plate and a carbon fibre reinforced carbon (C-C) plate where the C-C plates were 3.2 lower in stiffness than the stainless plates and both were implanted in adult male foxhounds and left for 24 weeks [41]. The results of this study showed that the loss of bone and decrease of mechanical properties beneath the plates were significantly higher with the more rigid stainless steel plates compared to the C-C plates [41]. The bones treated with stainless plates were 7% smaller in cross sectional area and had a modulus of elasticity 27% lower than those treated with C-C plates which corresponds to results of studies done by Uthoff et al., Comtet et al., Woo et al., and Tonino and Klopper as well [41].

This situation has created the need for finding low-stiffness material that would allow for a healthy bone healing at the fracture location while maintaining the two ends of the fractured bones firmly immobilized. If the bone callus material is assumed to be isotropic and homogenous the values of its Young's modulus can be reported as follows: 20 GPa for intact bone, 15 GPa for fractured bone at 75% healing, 10 GPa for fractured bone at 50% healing, and 0.01 GPa for fractured bone at 1% healing [42].

Benli et al calculated that a suitable Young's modulus of a low-stiffness plate material would be equal to 7.36 GPa compared to the Young's modulus of 110 GPa found in titanium alloy plates and 200 GPa in stainless-steel plates [37]. They performed numerical simulations of a bone fixation plate with a stiffness of 7.36 GPa under a compression stress of 2.5 MPa (for a patient weighing 80 kg) and found that the low-stiffness plate is capable of carrying the same

compressive load as metallic plates while increasing the portion of the load transferred to the fractured area which induces accelerated healing and leads to a healthier and stronger bone [37].

It is absolutely important that both the axial and bending stiffness of a low-stiffness composite plate is high enough to prevent excessive micro-movement at the fracture location which could jeopardize the healing process while being low enough for interfragmentary strains that would allow for a healthy healing process. Kim et al. performed a finite element analysis on the healing effect of bone plates made of carbon-epoxy (WSN3K) and glass-polypropylene (Twintex) composites. They found that Twintex composites bone plates ($[0]_{18}$), whose Young's modulus was 20 GPa in the axial direction, provided the most beneficial interfragmentary strain distribution and resulted in the highest healing rate [43]. In another study by Kim et al. on the effect of the flexural stiffness on a variety of carbon-epoxy composite plates ranging in axial stiffness from 70 GPa to 240 GPa, it was found that interfragmentary strain varied not only with the bending stiffness but also with the contact condition of the bone plate [44]. This necessitates that care should be taken in both of the selection of the material and the design of the plate to make sure that the composite plate allow for enough axial strain while limiting movement due to bending loads.

4. Methodology

The methodology used in this research work was mainly experimental but included some rough analytical estimations. The task at hand was to study the mechanical suitability of a flax-epoxy prepreg composite to be used in making implants for bone fixing surgery. Literature survey showed that the properties of flax fibre composites varied considerably depending on the type, source, and degree of processing of the flax fibres. This made it necessary to do our own in-house characterization of the flax-epoxy prepreg composite under study. Besides mechanical testing, parameters related to manufacturing had to be considered carefully. This included the parameters of curing cycle such as time, temperature and pressure which is explained in further details in the following sections.

4.1 Manufacturing

The absence of high quality manufacturing equipment for composite materials posed a real challenge to optimizing the manufacturing process. The manufacturing was done using a very small mould and a small industrial oven modified with a custom made hydraulic pressure system. This produced plates measuring 3" by 11" which were later cut using abrasive water jet technology to produce the test samples. This process was a limiting factor both qualitatively and quantitatively since it made it hard to produce a large number of samples in a short period of time or to accurately arrive at the optimal manufacturing pressure. For example, the manufacturer of the flax-epoxy prepreg specified 8 different possible curing cycles for the material, however, only three cycles, at the minimum, intermediate and maximum temperatures, were tested due to time limitations. The optimal pressure was decided experimentally by making a number of composite plates at different pressures and using visual inspection to decide which pressure yielded the most consolidated composite plates.

4.2 Testing

Testing of the composite flax-epoxy samples was limited to mechanical testing for the purpose of the characterization of the material. This consisted of tensile, flexural, and fatigue tests of samples made with different curing cycles and at different fibre orientations: unidirectional and two-directional. This helped define the basic material properties such as longitudinal and transverse strength, Young's Modulus, transverse modulus, shear modulus, and Poisson's ratio.

Most test samples were made of 16 layers which produced samples with the thickness of 3 mm except for a few samples which were made of 22 layers and had a thickness of 4 mm. The width and length of the test samples varied based on practical testing consideration and ASTM standard recommendations for polymer matrix composite materials: D3093/D3093M - 08 (tensile), D7264/D7264M - 07 (flexural) and D3479/D3479M - 96 (fatigue).

4.3 Implant Design and Optimization

Mechanical characterization was used to design a prototype of a bone fixation plate using rough analytical estimations. The design variables were thickness (number of layers), width and orientation of layers. Since the fibre-epoxy implant was to be compared with metallic implants it was decided that its thickness and width (i.e. cross sectional area) should be identical to those made of metals or other composites (carbon etc.). The thickness of the design implant was 4 mm which was achieved by using 22 layers. It was necessary to take into account not only longitudinal and bending loads but also shear loads. Therefore, the composite implants were designed to be made of about 65% unidirectional fibres (in the direction of the axial load) and 35% fibres oriented at plus and minus 45 degrees. This configuration was found, based on analytical estimations, to provide suitable resistance in the longitudinal direction while providing some resistance against in-plane shear loads. The design needed to strictly meet the following criteria: a Young's modulus and flexural modulus close to that of the human bone and satisfactory strength and stiffness for bearing both the static and dynamic loads. For this purpose the design was subjected to static tensile and bending testing as well as dynamic fatigue testing. The implant design was not found to have sufficient flexural strength and an alternative optimized design was suggested.

5. Manufacturing

Manufacturing test samples followed two major steps: layout and curing. The flax-epoxy prepreg came in a big roll that had to be maintained in a frozen state to prevent the epoxy from curing over time at room temperature.

5.1 Layout

Individual layers were cut out of the prepreg roll in the desired fibre direction. Layout of the layers followed according to the desired design (unidirectional, transverse, quasi-isotropic etc.). The mould was cleaned and covered with the release agent and eventually the composite was placed in the mould which was put in the oven and subjected to the desired pressure. Photos of the layout process are shown in Figure 1 to Figure 7.

5.2 Curing

Two of the curing cycles specified by the manufacturer (at the maximum and minimum temperatures) were tested for the purpose of comparison. In the first one the curing was done at 110°C for 2 hours and in the second one at 150°C for 30 minutes. In addition, a third curing cycle was tested where a number of cycles were combined to produce plates cured at an intermediate temperature. The ramping of temperature was done at 2°C degree per minute and pressure was applied using the custom made system. The appropriate pressure was decided by trial and error where the manufactured samples were inspected visually for the appropriate level of consolidation and the optimal pressure for 16-layer composites (majority of the samples were made of 16 layers) was found to be in the range of 3.5 to 4 bars.



Figure 1: Mapping and cutting of prepreg composite layers

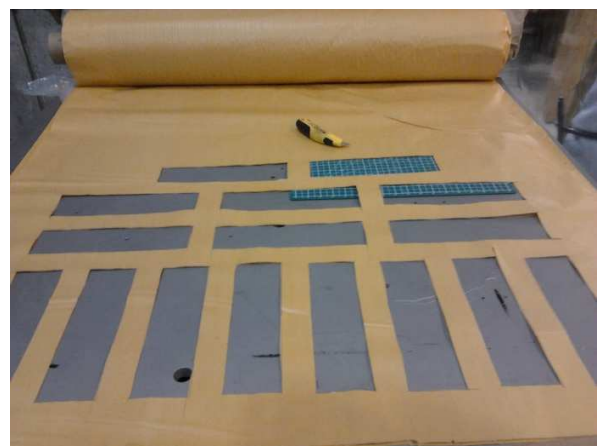


Figure 2: Composite role with layers cut out



Figure 3: Composite layers before lay-up



Figure 4: Lay-out of composite layers



Figure 5: Preparation of the mould



Figure 6: Composite plate inside the mould



Figure 7: Pressure system inside the oven

6. Testing

The majority of testing consisted of tensile testing, however, flexural tests and fatigues testing were done as well. All in all 57 samples were tested and their results were analyzed. Two different machines were used, one for static tensile and bending testing and another for fatigue testing.

6.1 Tensile Test

Tensile tests were performed on unidirectional, transverse, and two-directional samples cured at three different temperatures: 110°C, 150°C and an intermediate temperature between 110°C and 150°C. The tested samples consisted of 21 unidirectional samples ($[0]_{16}$), 6 transverse samples ($[90]_{16}$), 5 symmetrical $[0,90]_{8S}$ samples, 5 symmetrical ($[+45,-45]_{8S}$) samples, 4 isotropic ($[0,45,90,-45]_{4S}$) samples, 2 symmetrical $[+45,-45]$ samples, and 3 symmetrical samples with a $[0,0,0,45,0,-45,0,\dots]_{2S}$ configuration. All samples were made of 16 layers except for the last 3 which consisted of 22 layers. The tensile tests were done on a UNITED machine linked to computer system with a DATUM software to collected test data. The testing speed was 2 mm/min and an extensometer was used to measure elongation. A 50 kN load cell was used in all the tensile tests. In a few samples, strain gauges in the transverse direction were used together with the extensometer in order to find the Poisson's ratio and shear modulus. Photos of the tensile test are given in Figure 8 to Figure 11.



Figure 8: UNITED tensile test machine



Figure 9: A view of the grips used for tensile testing



Figure 10: Tensile test with extensometer - close view



Figure 11: Tensile testing with extensometer

6.2 Bending Test

Three-point bending tests were performed on unidirectional and two-directional samples cured at two different temperatures: 110° C and 150° C. Tested samples consisted of 7 unidirectional samples of 16 layers each and 3 symmetrical samples with a $[0,0,0,+45,0,-45,0\dots]_{2S}$ configuration of 22 layers each. The bending tests were also done on the UNITED machine connected to computer system with the DATUM software. The testing speed was 0.5 in/min and a 500 N load cell was used in all the bending tests. Photos of the bending test are given in Figure 12 to Figure 15.



Figure 12: Bending test - close view



Figure 13: Bending test



Figure 14: Bending test - near the end of test side view

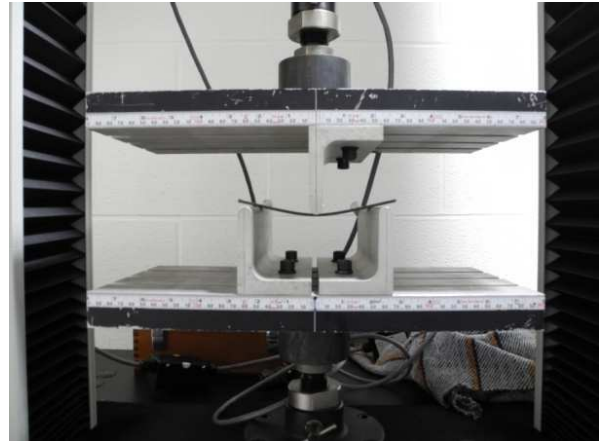


Figure 15: Bending test - near the end of test

6.3 Fatigue Test

Fatigue testing was done on 3 samples with a $[0,0,0,+45,0,-45,0\dots]_{2S}$ configuration, made of 22 layers and cured at $110\text{ }^{\circ}\text{C}$. Dynamics loading was set at 33%, 50%, and 65% of the maximum static failure load found previously from tensile testing. The fatigue test was done in tension-tension with a frequency of 10 Hz on a hydraulic machine connected to computer software for control and data collection. Photos of the test are shown in Figures 16 and 17.

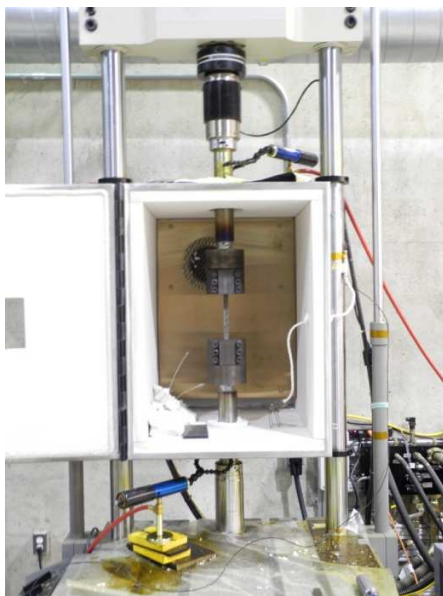


Figure 16: Fatigue testing



Figure 17: Fatigue testing - close view

7. Results

7.1 Tensile Test Results

Summary of tensile test results of unidirectional samples made of 16 layer and cured at different temperatures is given in Table 1.

Table 1: Longitudinal tensile test results of unidirectional samples

Sample Number	Width	Thickness	Area	Curing Temperature	Failure Load	Ultimate Tensile Strength	Failure Strain	Young's Modulus
	mm	mm	mm ²	°C	kN	MPa	%	GPa
T1	15.5	2.74	42.6	110	11.8	276	1.21	20.6
T2	15.5	3.14	48.8	110	14.2	291	1.28	20.8
T3	15.3	3.06	46.8	110	14.1	301	1.28	21.6
T4	15.6	3.02	47.2	110	14.1	298	1.23	22.1
T5	15.0	3.15	47.4	110	12.6	266	1.10	21.5
T6	15.5	2.66	41.2	110	12.7	308	1.26	21.9
T7	15.5	3.38	52.4	110	11.2	225	1.39	13.5
T8	15.5	3	46.5	150	14.5	312	1.13	25.6
T9	13.8	3.16	43.6	150	12.4	283	1.38	18
T10	15.7	2.88	45.1	150	15.4	342	1.34	23
T11	15.0	3.21	48.1	150	14	291	1.06	21.6
T15	15.4	2.95	45.5	150	13.6	299	1.07	25.9
T16	15.5	3.06	47.3	150	14.3	313	1.12	25.3
T17	15.4	3.03	46.6	150	13.9	306	1.10	25.7
A1	26.1	2.97	77.5	Intermediate	27.7	358	1.47	22.4
A2	24.8	2.92	72.4	Intermediate	25.6	353	1.59	22.6
A3	26.2	2.88	75.3	Intermediate	21.9	291	1.28	21.9
A4	24.8	2.90	71.9	Intermediate	24.2	336	1.39	25.2
A5	24.8	2.90	71.9	Intermediate	25.8	359	1.60	22.2

The ultimate tensile strength, maximum strain, and Young's modulus of all the unidirectional samples tested in the longitudinal direction are given in Figure 18 to Figure 20. Further discussion of these results is found in the Discussion section.

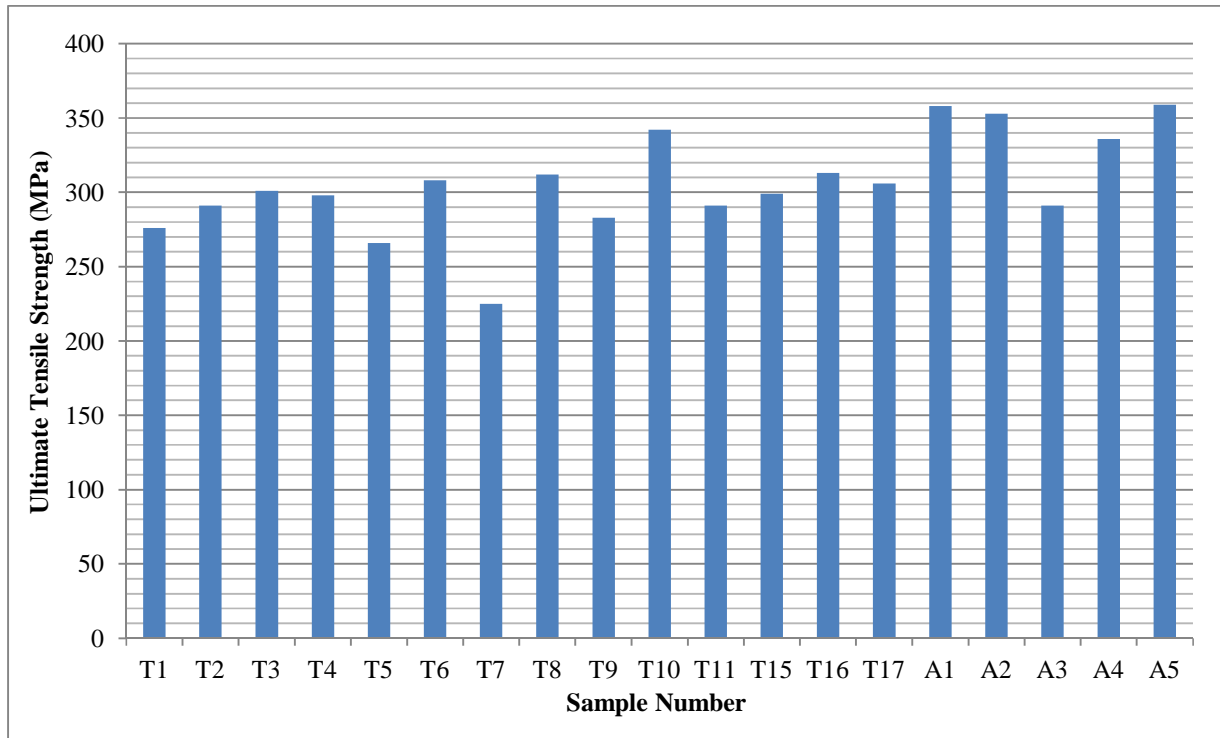


Figure 18: Ultimate strength of unidirectional samples

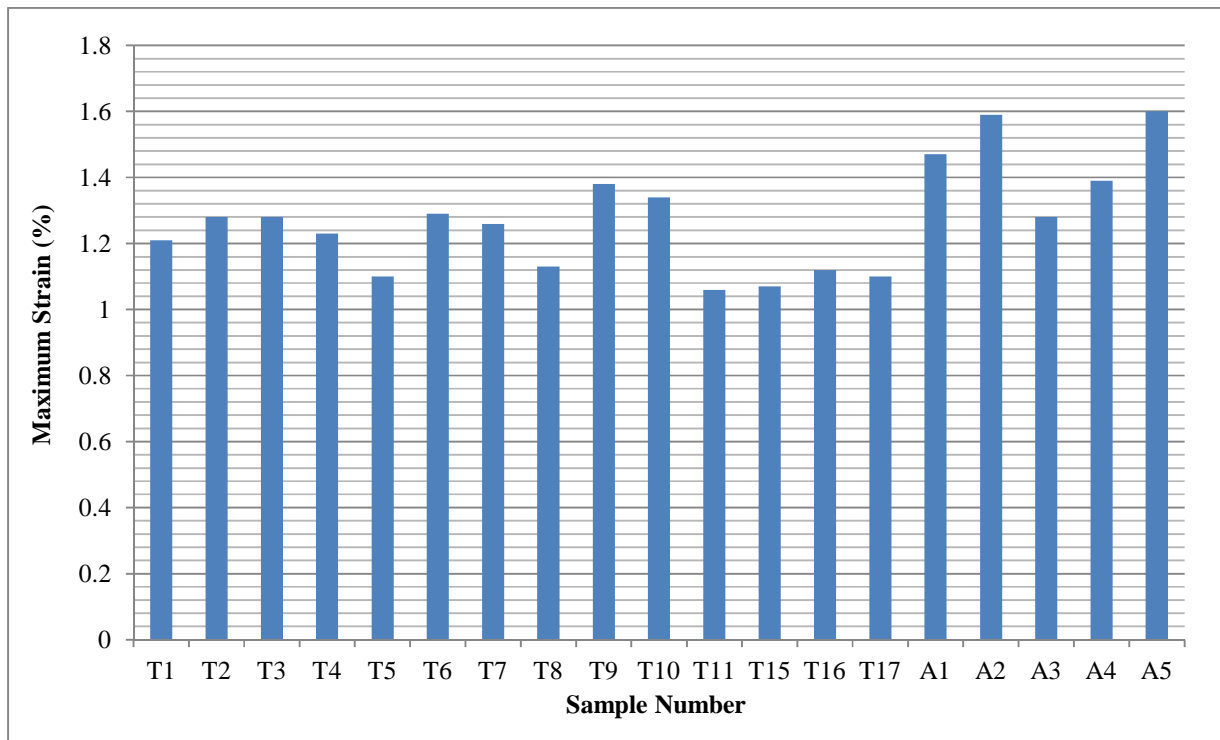


Figure 19: Maximum strain of unidirectional samples

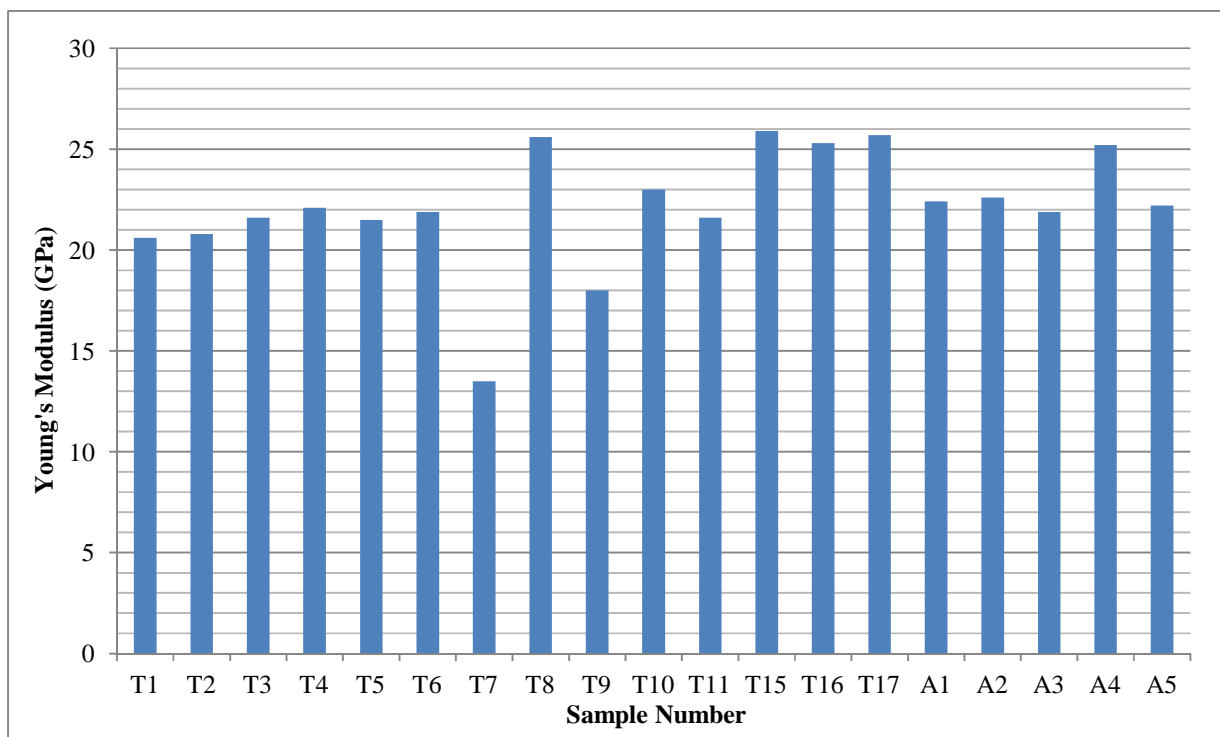


Figure 20: Young's modulus values of unidirectional samples

Summary of transverse test results of unidirectional samples made of 16 layer and cured at two different temperatures is given in Table 2.

Table 2: Transverse tensile test results of unidirectional samples

Sample Number	Width	Thickness	Area	Curing Temperature	Failure Load	Transverse Strength	Failure Strain	Transverse Modulus
	mm	mm	mm ²	°C	kN	MPa	%	GPa
T18	19.5	3.06	59.5	150	1.595	26.8	0.866	4.36
T19	19.1	3.07	58.7	150	1.551	26.4	0.76	4.28
T20	18.9	3.22	60.7	150	1.779	29.3	0.864	4.99
T21	18.7	3.00	56.0	110	1.083	19.3	1.16	2.78
T22	20.0	3.03	60.7	110	1.193	19.7	1.12	3.31
T23	18.5	3.02	55.7	110	0.990	16.3	1.13	2.47

Summary of longitudinal test results of two unidirectional samples cured at different temperatures and aimed at finding the Poisson ratio of the material is given in Table 3. Summary of test results of two plus and minus 45 samples aimed at finding the shear modulus is given in Table 4.

Table 3: Poisson's ratio at different curing temperatures

Sample Number	Width	Thickness	Area	Curing Temperature	Poisson's Ratio
	mm	mm	mm ²	°C	GPa
P1	14.8	3.17	46.9	150	0.31
P2	16.9	3.06	49.2	110	0.36

Table 4: Shear modulus

Sample Number	Width	Thickness	Area	Number of Layers	Curing Temperature	Shear Modulus
	mm	mm	mm ²		°C	GPa
S1	25.2	3.65	92.126	20	150	2.27
S2	24.6	3.06	75.3372	16	150	1.67

The ultimate transverse strength, failure strain, and transverse modulus of all the unidirectional samples tested in the transverse direction are given in Figure 21 to Figure 23. Further discussion of the results is found in the Discussion section.

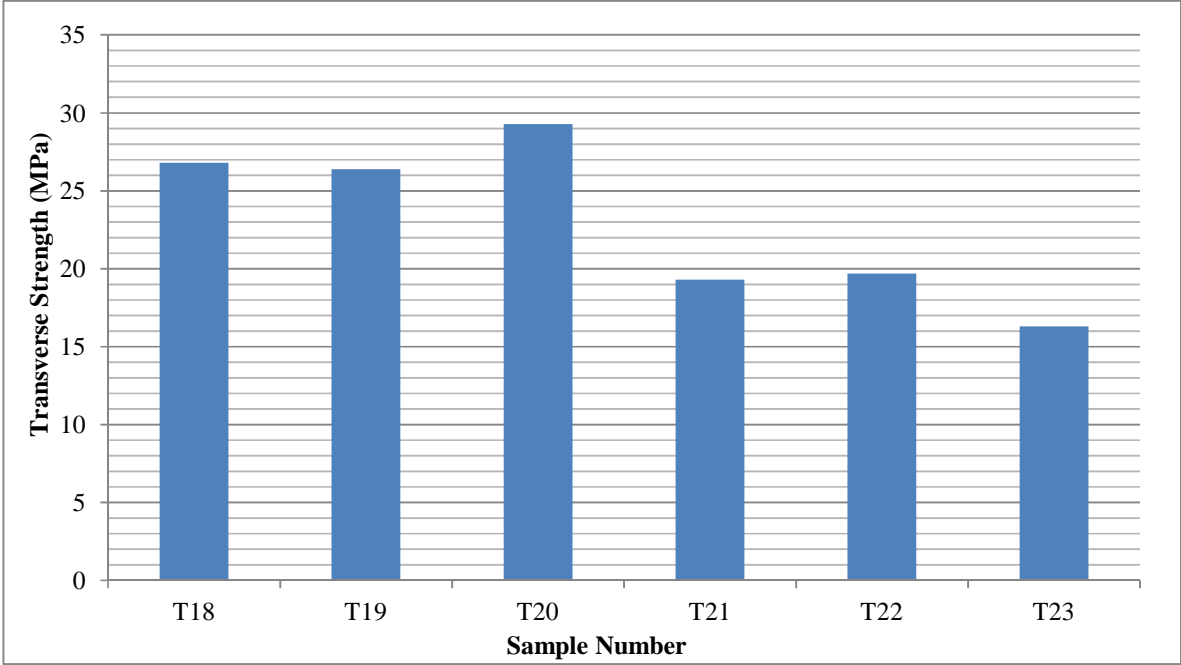


Figure 21: Transverse strength of unidirectional samples

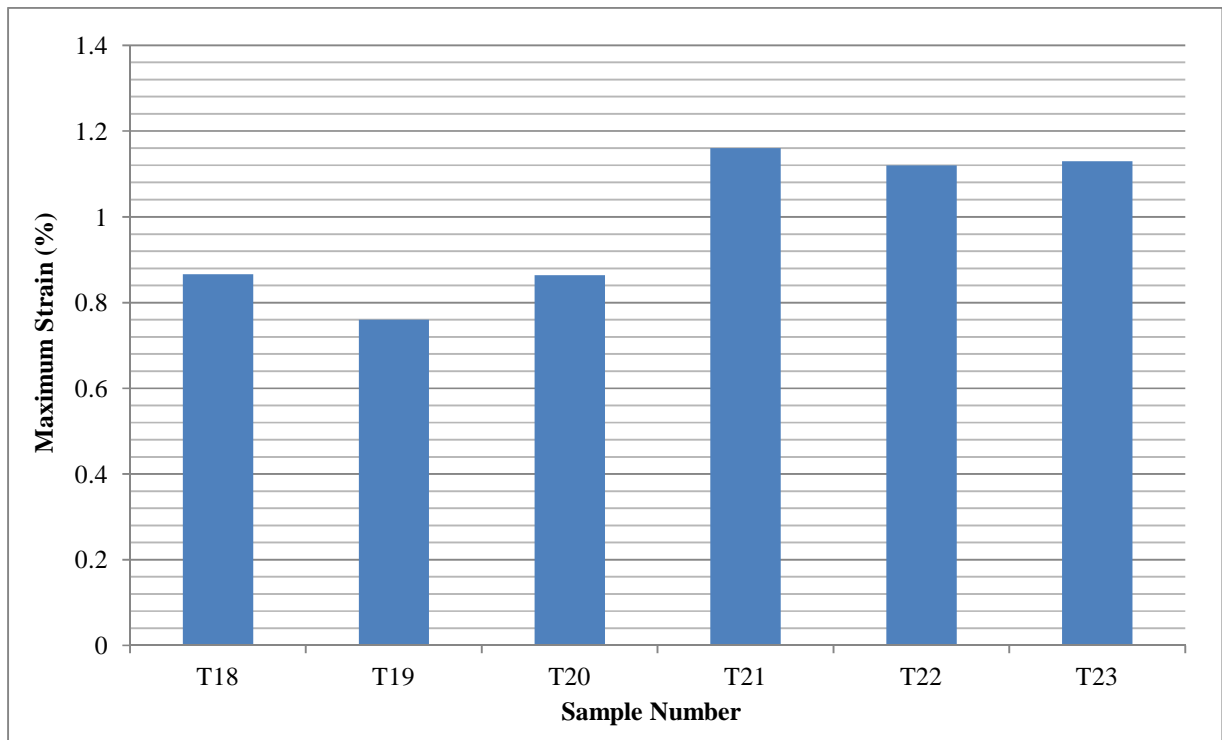


Figure 22: Maximum transverse strain of unidirectional samples

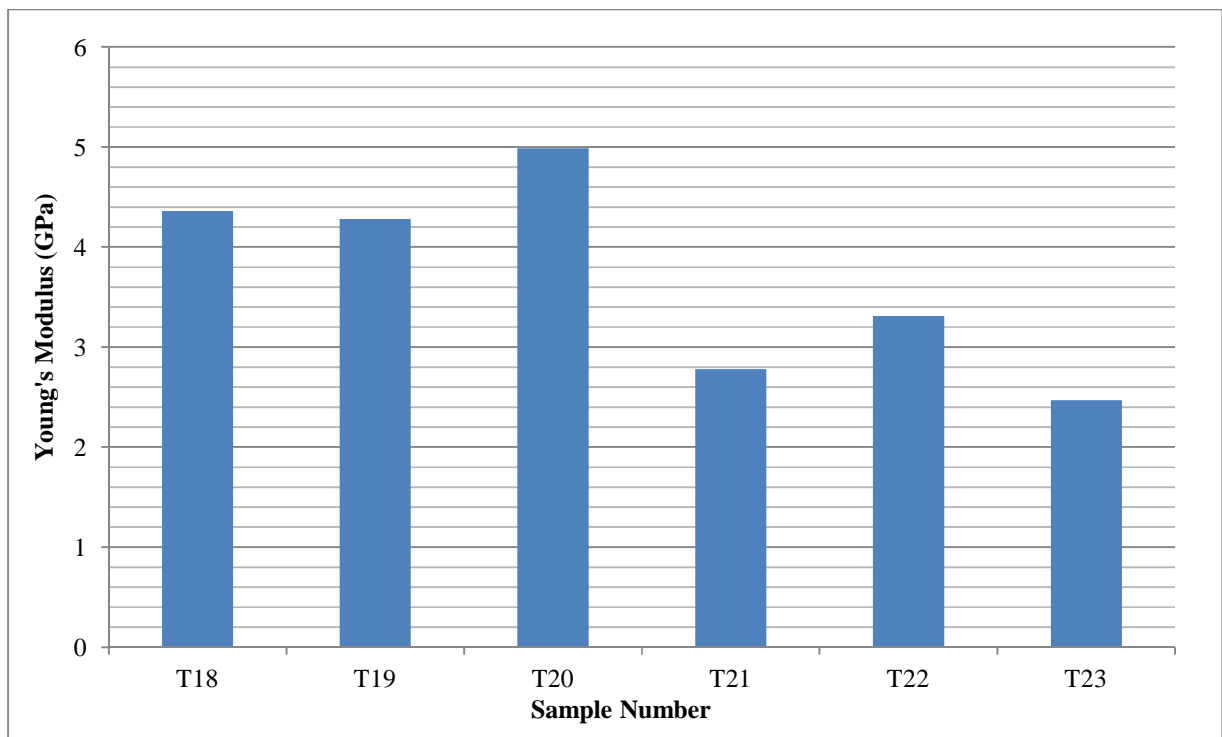


Figure 23: Transverse Young's modulus of unidirectional samples

Summary of tensile test results of unidirectional and two-directional samples made of 16 layer and cured at an intermediate temperature between 110 °C and 150 °C is given in Table 5. Tensile test results of design samples made of 22 layers cured at 110 °C is given in Table 6.

Table 5: Tensile test results of unidirectional and two-directional samples

Sample Number	Width	Thickness	Area	Orientation	Failure Load	Ultimate Tensile Strength	Maximum Strain	Young's Modulus
	mm	mm	mm ²		kN	MPa	%	GPa
A1	26.1	2.97	77.5	[0] ₁₆	27.7	358	1.47	22.4
A2	24.8	2.92	72.4	[0] ₁₆	25.6	353	1.59	22.6
A3	26.2	2.88	75.3	[0] ₁₆	21.9	291	1.28	21.9
A4	24.8	2.9	71.9	[0] ₁₆	24.2	336	1.39	25.2
A5	24.8	2.9	71.9	[0] ₁₆	25.8	359	1.60	22.2
A6	26.2	2.99	78.3	[0,90] _{8s}	12.4	158	1.03	11.8
A7	24.7	2.92	72.1	[0,90] _{8s}	11.9	165	1.25	10.5
A8	26.2	3.07	80.3	[0,90] _{8s}	13.6	170	1.42	10.0
A13	26.2	3.07	80.3	[0,90] _{8s}	14.7	184	1.42	10.3
A14	24.8	3.04	75.3	[0,90] _{8s}	13.6	180	1.47	10.4
A9	24.8	2.93	72.8	[0,+45,90,-45] _{4s}	10.4	143	1.38	8.00
A10	26.1	2.85	74.4	[0,+45,90,-45] _{4s}	10.8	145	1.40	7.90
A15	26.2	2.9	76.1	[0,+45,90,-45] _{4s}	12.9	170	1.53	9.00
A16	24.9	3.1	77.2	[0,+45,90,-45] _{4s}	12.1	156	1.80	7.90

Table 6: Tensile test results of design samples

Sample Number	Width	Thickness	Area	Orientation	Failure Load	Ultimate Tensile Strength	Failure Strain	Young's Modulus
	mm	mm	mm ²		kN	MPa	%	GPa
T12	15.5	4.2	65.0	[0,0,0,+45,0,-45,0,.....] _{11s}	11.9	186	1.18	8.10
T13	15.6	4.11	64.2	[0,0,0,+45,0,-45,0,.....] _{11s}	13.6	209	1.26	14.5
T14	15.7	4.21	65.9	[0,0,0,+45,0,-45,0,.....] _{11s}	13.6	206	1.20	15.0

The ultimate tensile strength, maximum strain, and Young's modulus of all the unidirectional and two-directional samples cured at an intermediate temperature and tested in the longitudinal direction are given in Figure 24 to Figure 26. Further discussion of these results is found in the Discussion section.

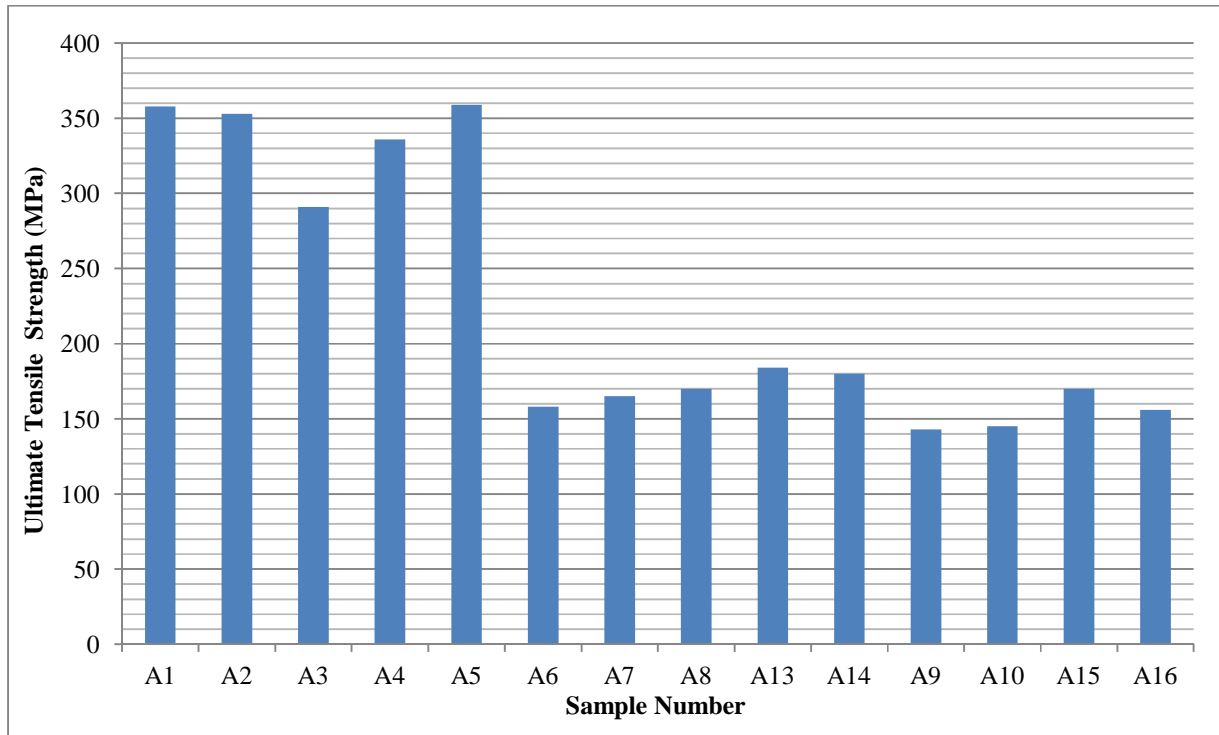


Figure 24: Ultimate tensile strength of composites with different ply orientation

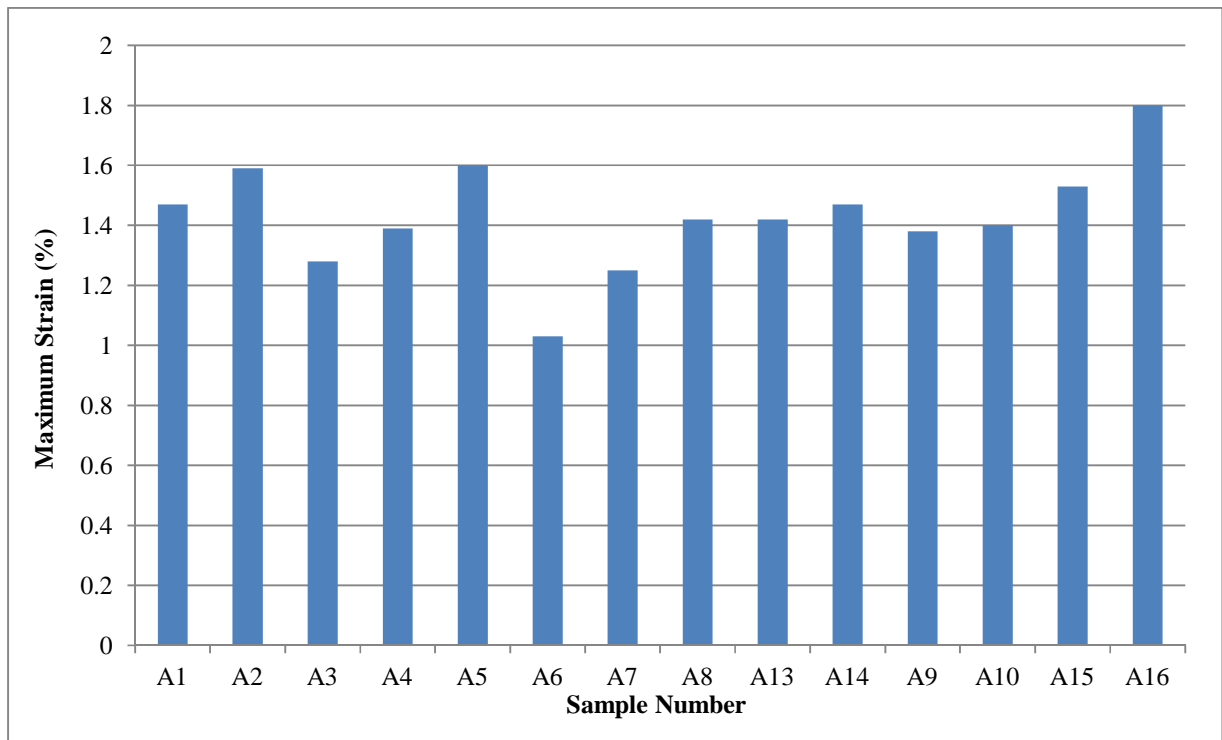


Figure 25: Maximum strain of composites with different orientation

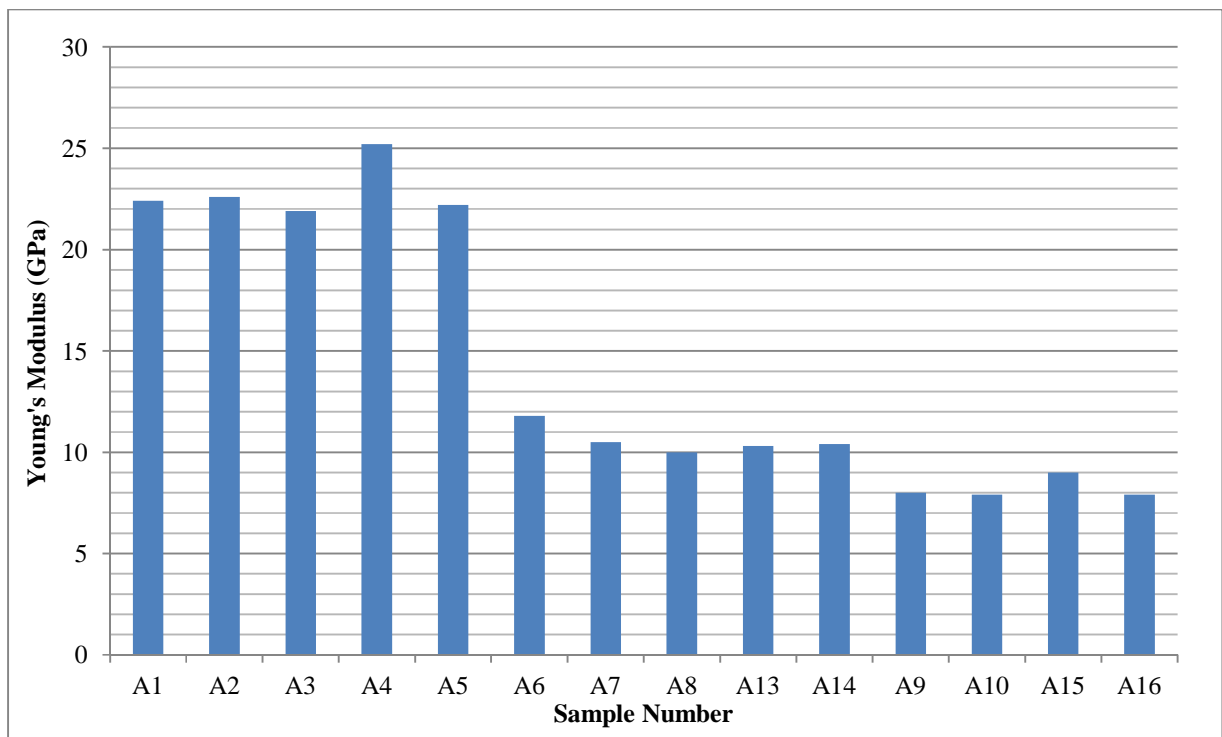


Figure 26: Young's modulus of composites with different ply orientation

The ultimate tensile strength, maximum strain, and Young's modulus of the three design samples cured at 110 °C temperature and tested in the longitudinal direction is given in Figure 27 to Figure 29. Further discussion of these results is found in the Discussion section.

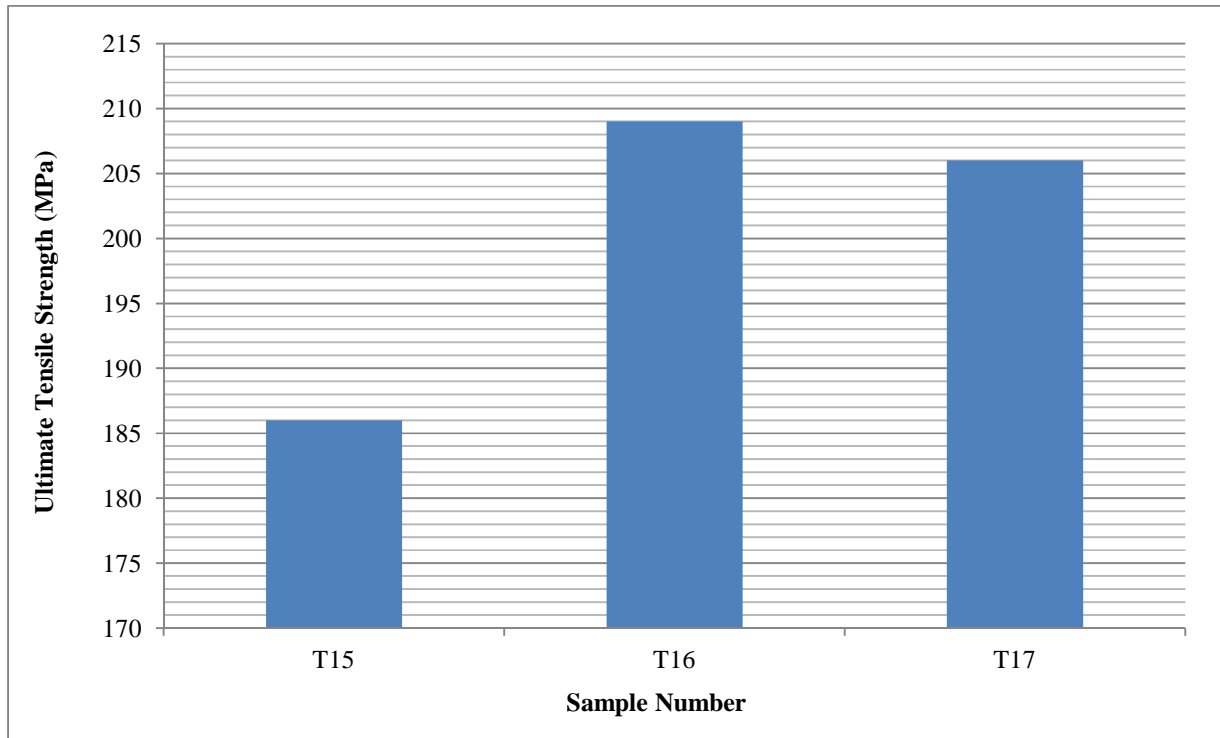


Figure 27: Tensile strength of design samples

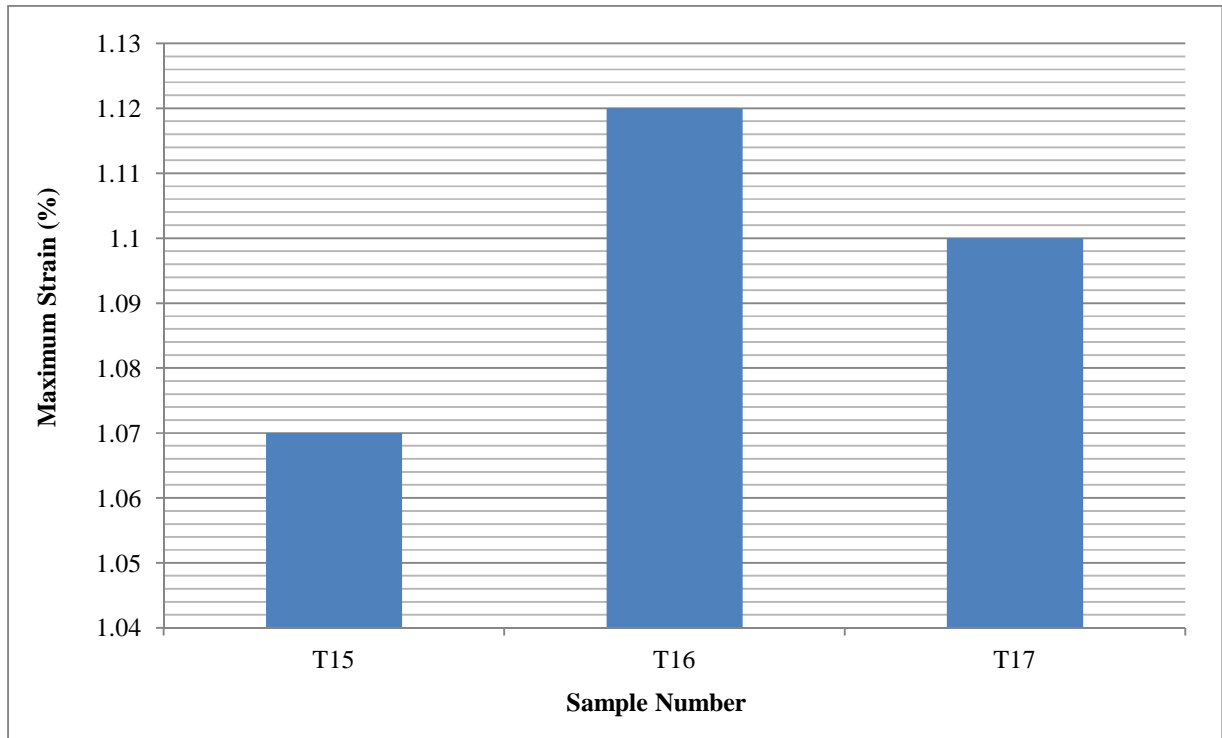


Figure 28: Maximum strain of design samples

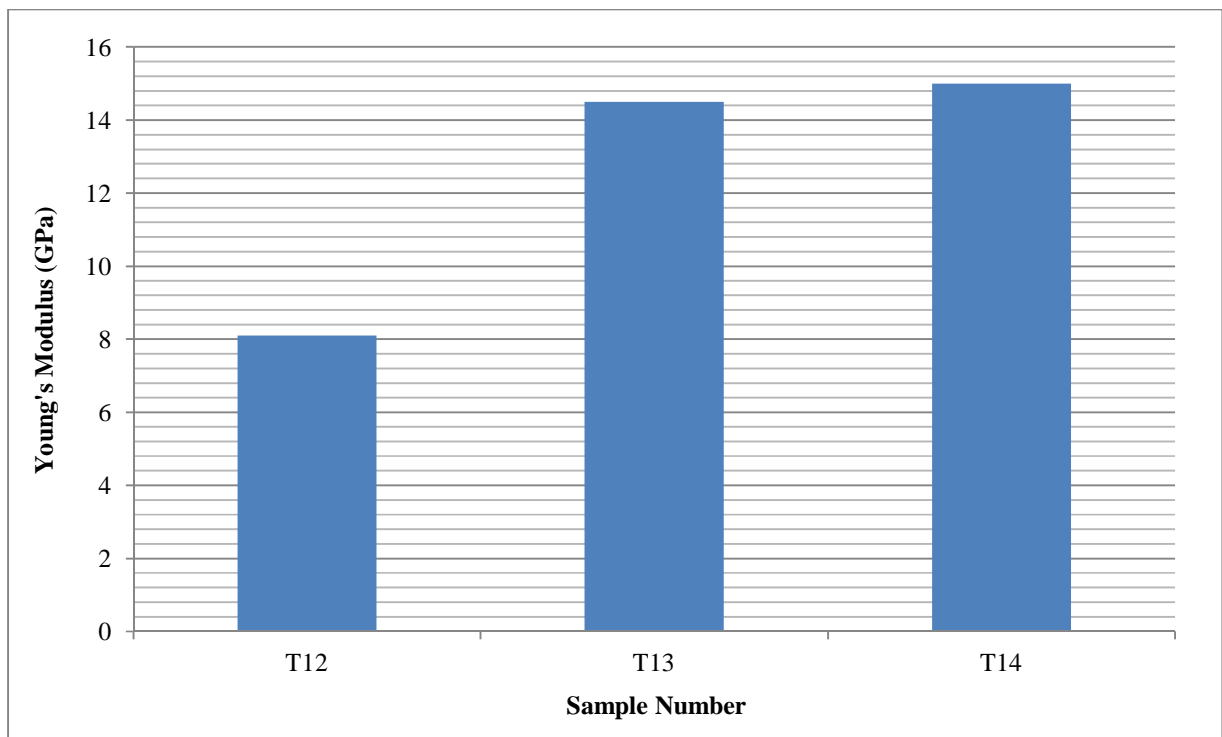


Figure 29: Young's modulus of design samples

Graphs showing the tensile behaviour of unidirectional samples T4 (cured at 110 °C) and T17 (150 °C) and design sample T13 are given in Figure 30 to Figure 35 in which stress is plotted against strain. Further discussion of these graphs is found in the Discussion section.

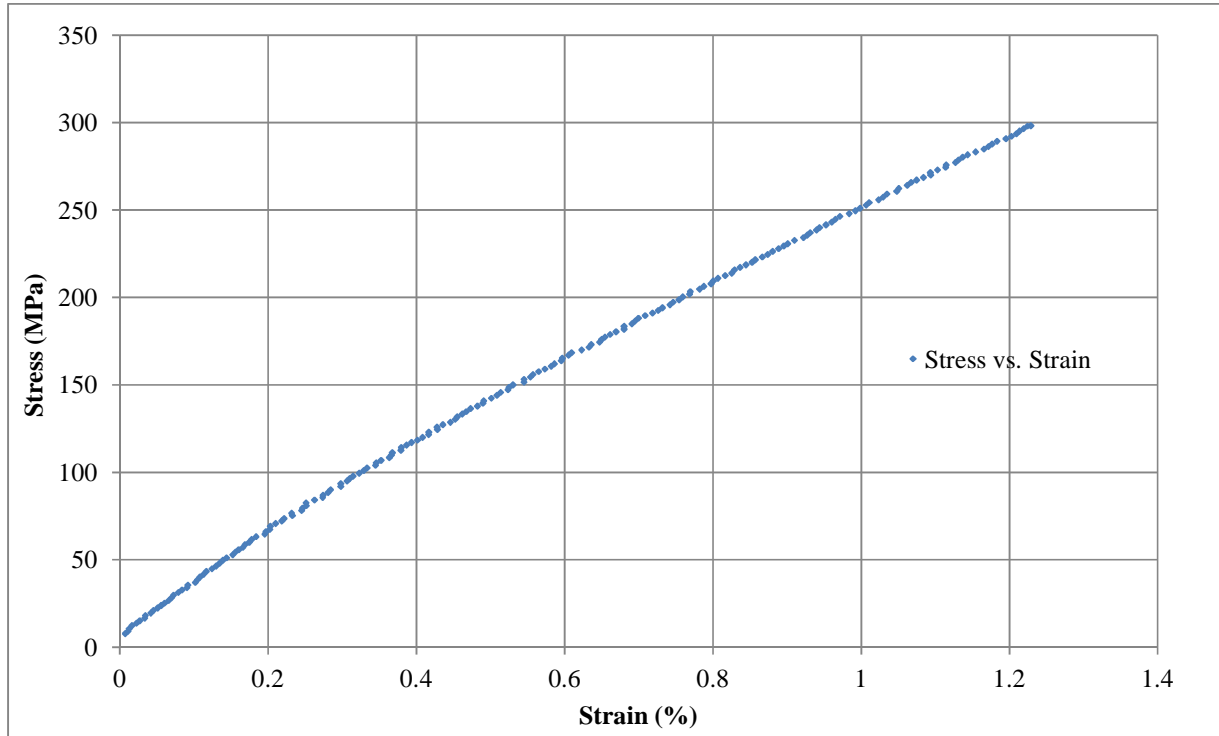


Figure 30: Tensile behaviour of unidirectional sample T4 cured at 110 °C

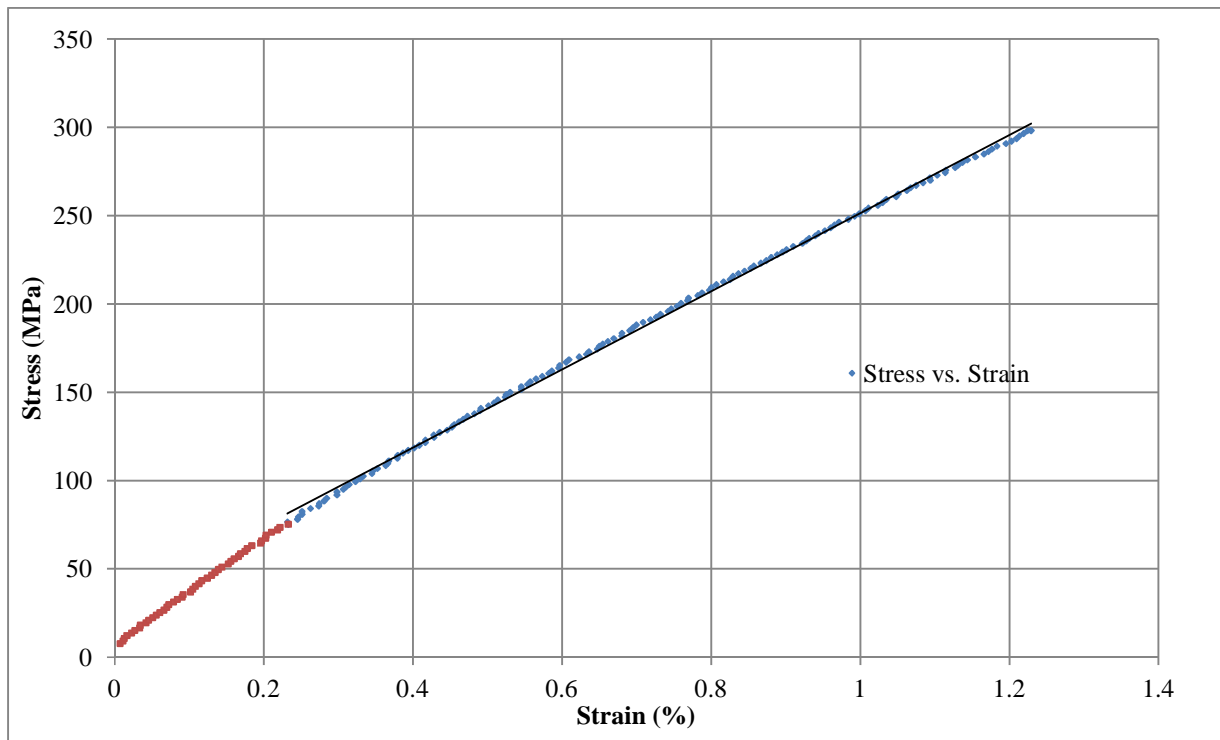


Figure 31: Young's Modulus of unidirectional sample T4 cured at 110 °C

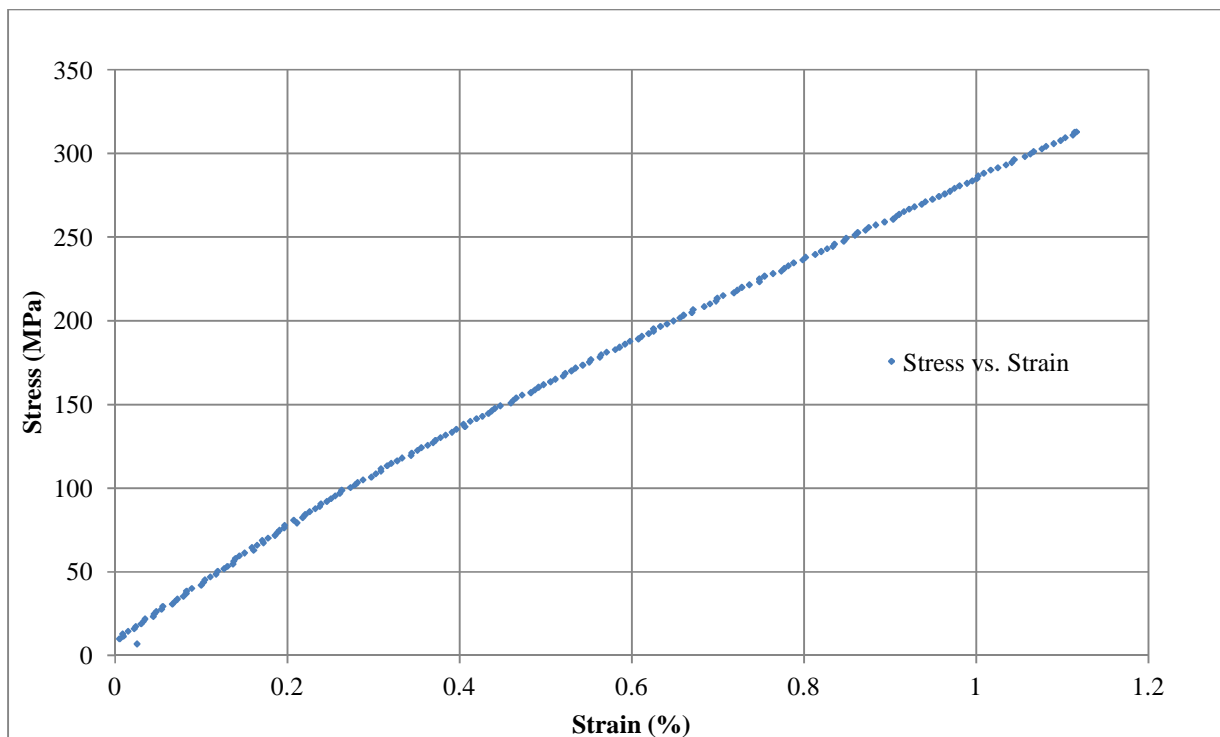


Figure 32: Tensile behaviour of unidirectional sample T17 cured at 150 °C

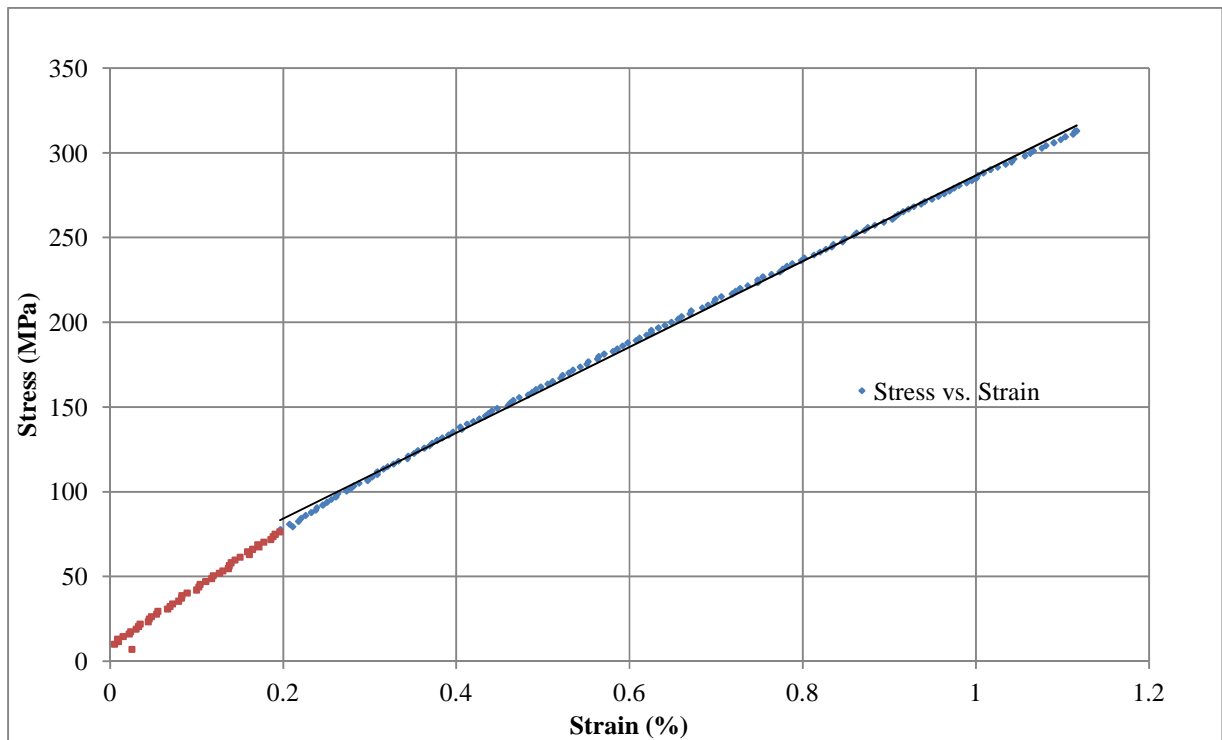


Figure 33: Young's modulus of unidirectional sample T17 cured at 150 °C

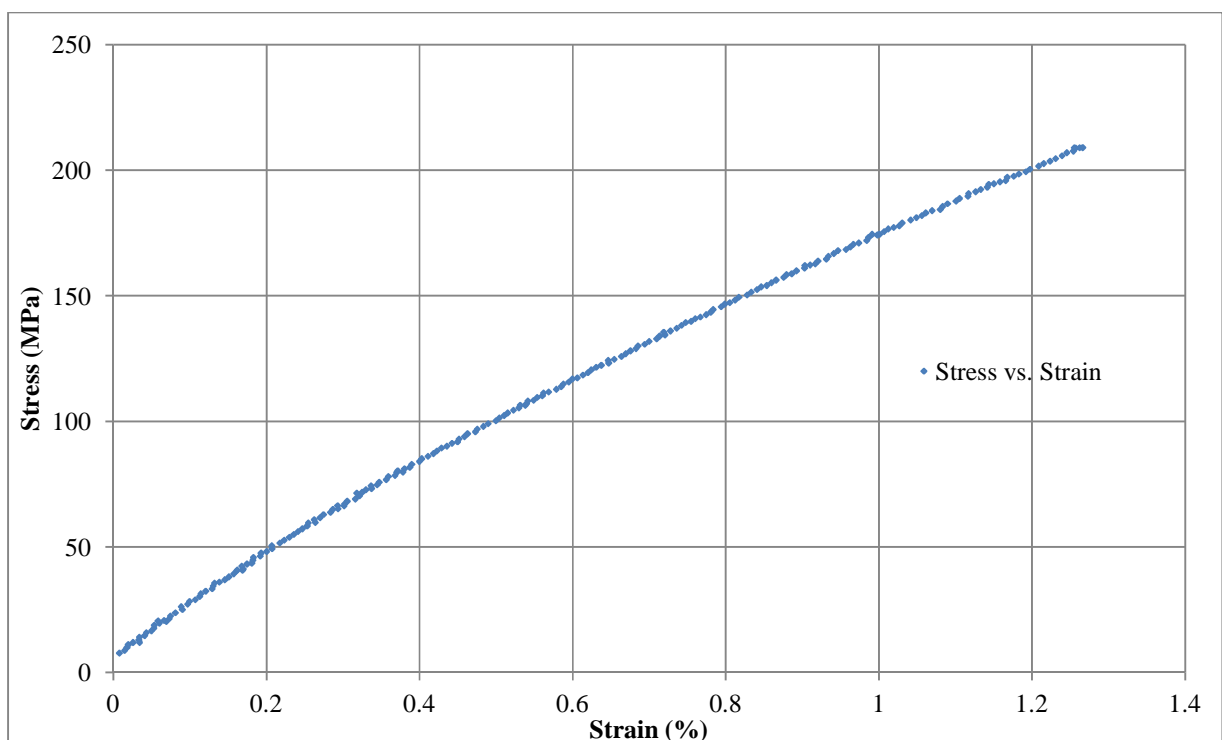


Figure 34: Tensile behaviour of design sample T13 cured at 110 °C

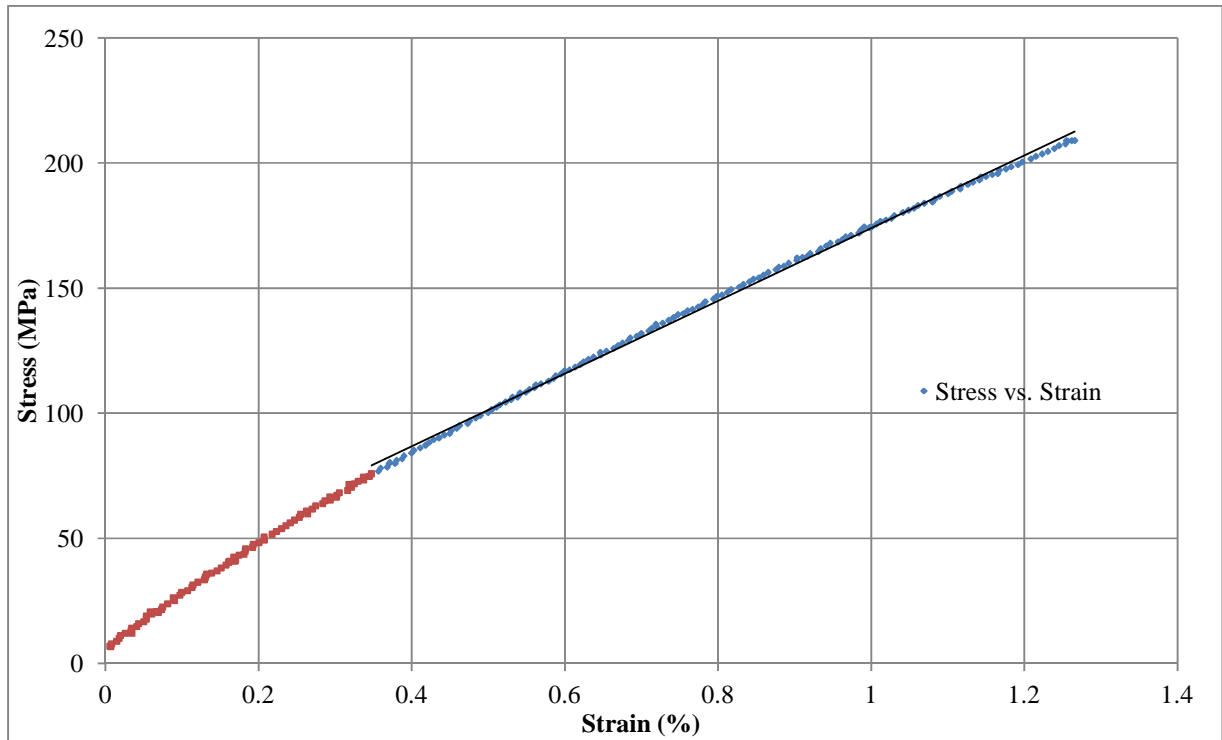


Figure 35: Young's modulus of design sample T13 cured at 110 °C

Graphs showing the tensile transverse behaviour of unidirectional samples T22 (cured at 110 °C) and T18 (150 °C) are given in Figure 36 to Figure 39 in which stress is plotted against strain. Further discussion of these graphs is found in the Discussion section.

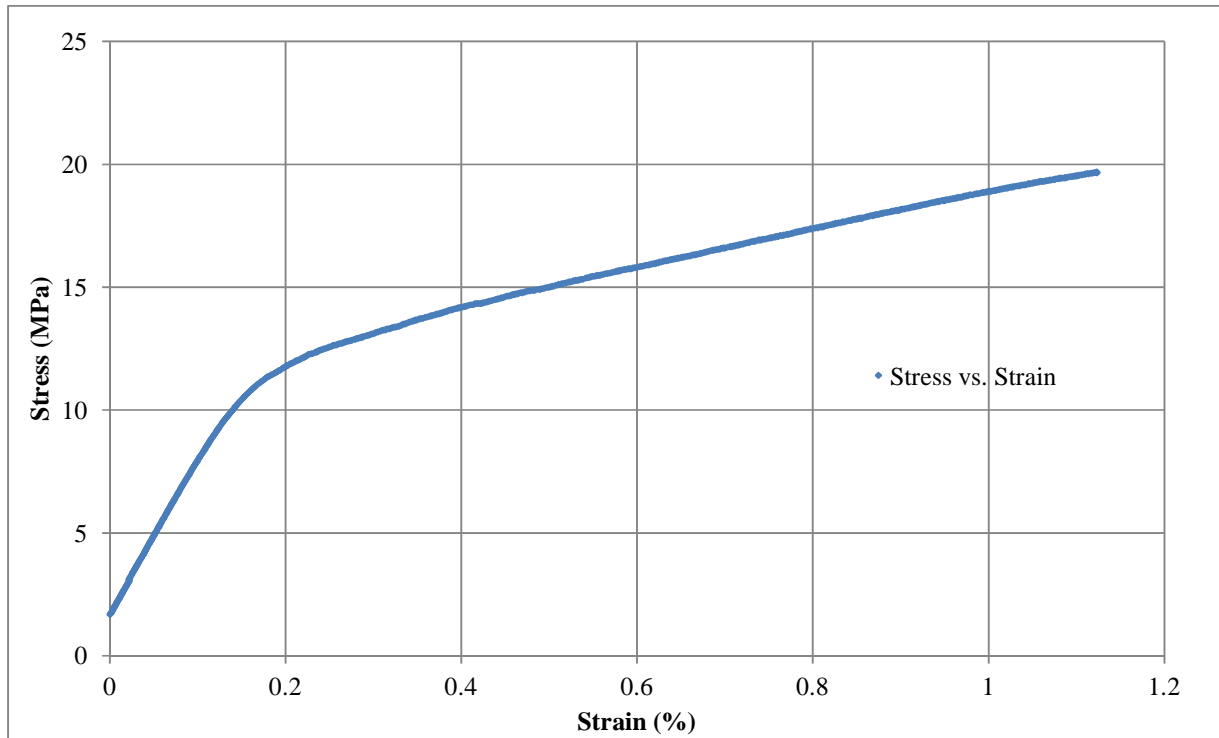


Figure 36: Transverse behaviour of unidirectional sample T22 cured at 110 °C

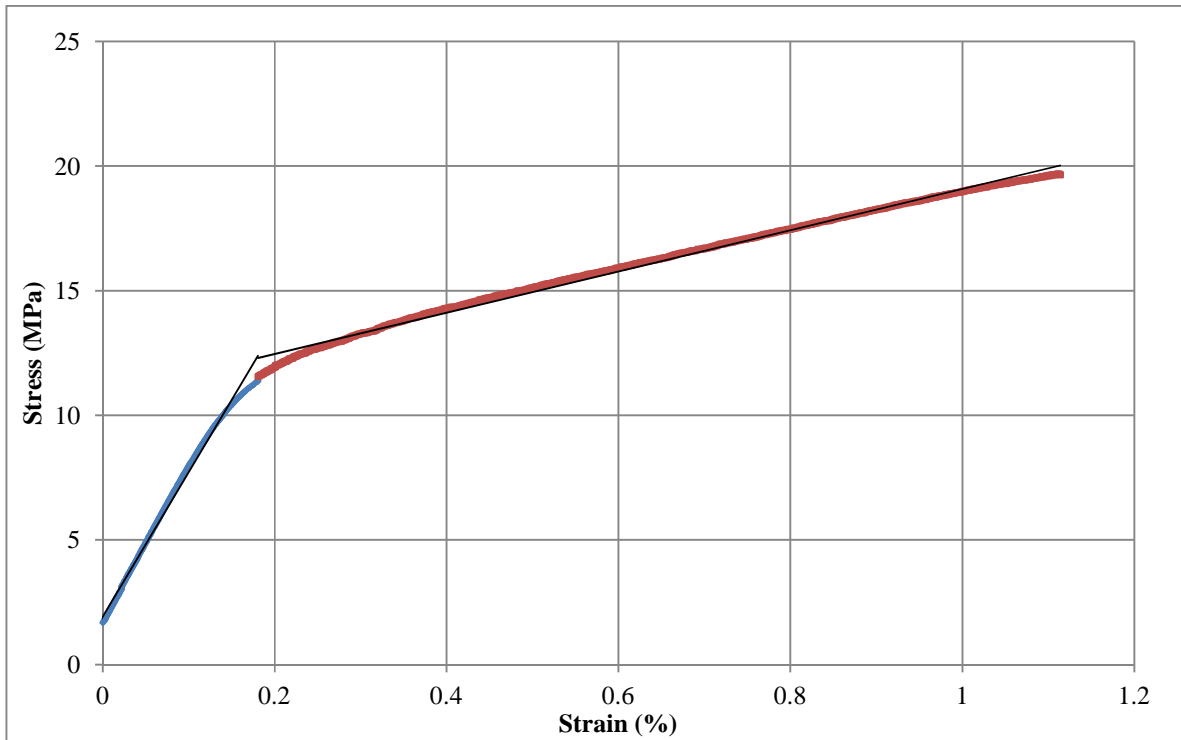


Figure 37: Transverse modulus of unidirectional sample T22 cured at 110 °C

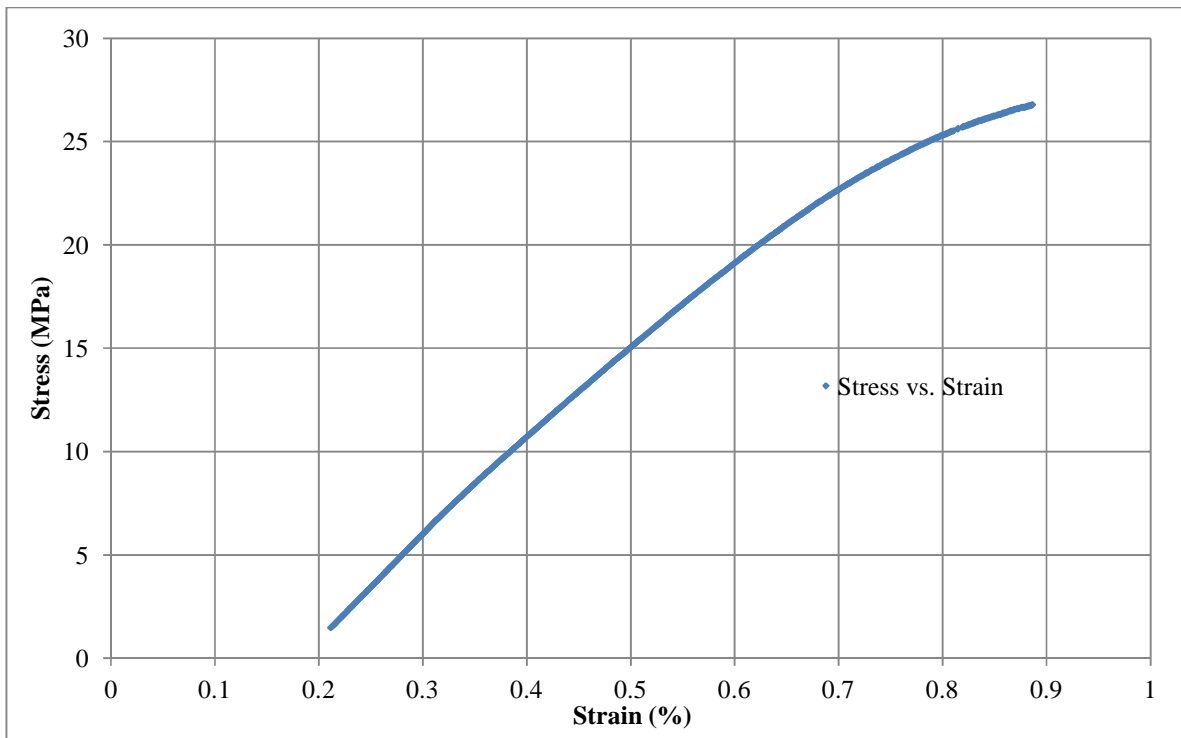


Figure 38: Transverse behaviour of unidirectional sample T18 cured at 150 °C

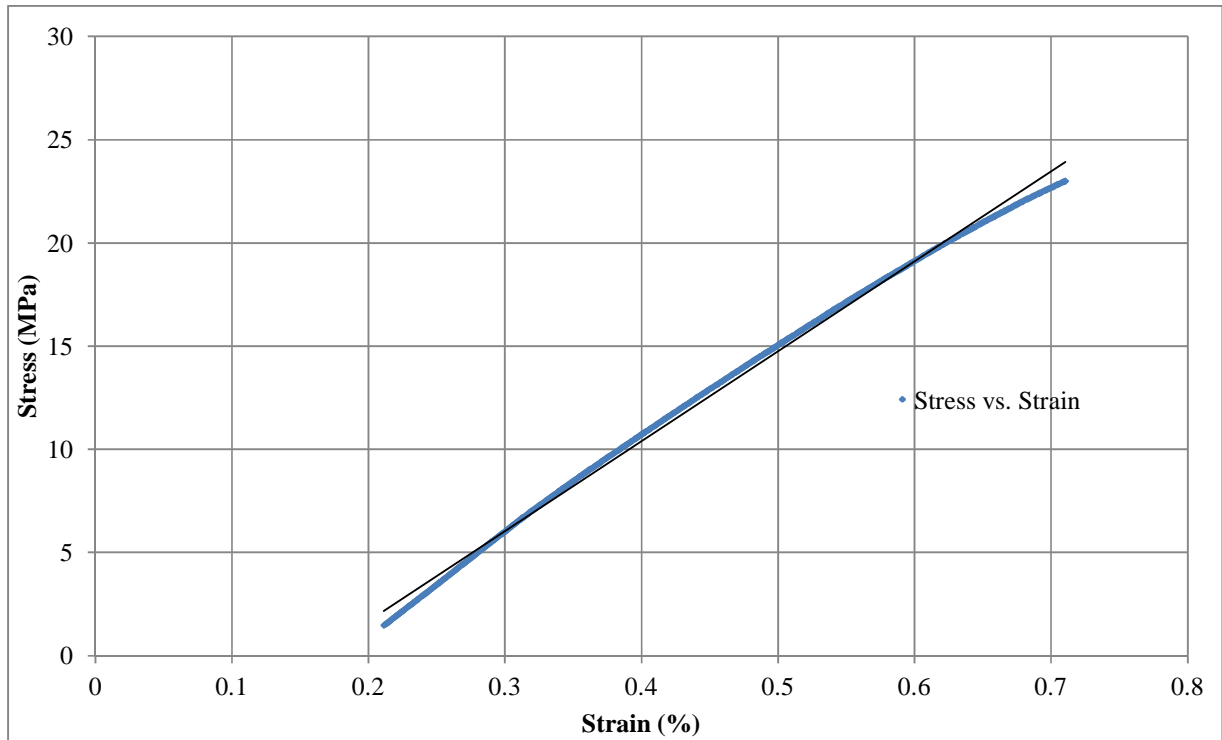


Figure 39: Transverse modulus of unidirectional sample T18 cured at 150 °C

7.2 Bending Test Results

Summary of bending test results of all 16-layer unidirectional samples cured at 110 °C and 150 °C is given in Tables 7 and 8.

Table 7: Bending test results for unidirectional samples

Sample Number	Width	Thickness	Area	Curing Temperature	Failure Load	Ultimate Surface Strength	Maximum Deflection	Max outer surface Strain
	mm	mm	mm ²		N	MPa	mm	%
B4	15.4	3.02	46.57	110	203	260	16.1	2.03
B5	15.7	2.98	46.7	110	208	269	13.9	1.73
B6	15.6	3.21	50.1	110	179	200	9.15	1.22
B7	15.3	2.78	42.5	110	87.4	133	5.93	0.687
B8	15.7	3.01	47.3	150	250	316	12.3	1.54
B9	15.0	3.09	46.2	150	223	260	10.5	1.35
B10	15.3	3.02	46.1	150	258	333	12.1	1.52

Table 8: Regional and average flexural modulus values for unidirectional samples

Sample Number	Width	Thickness	Area	Curing Temperature	Initial Flexural Modulus	Middle Flexural Modulus	Final Flexural Modulus	Average Flexural Modulus
	mm	mm	mm ²		GPa	GPa	GPa	GPa
B4	15.4	3.02	46.57	110	27.2	15.7	6.12	16.5
B5	15.7	2.98	46.7	110	28.5	16.5	6.98	17.3
B6	15.6	3.21	50.1	110	28	16.1	6.95	17
B7	15.3	2.78	42.5	110	23.2	12.3	-	-
B8	15.7	3.01	47.3	150	27.1	-	11.5	22.3
B9	15.0	3.09	46.2	150	26.4	-	8.19	23.5
B10	15.3	3.02	46.1	150	28.4	-	12.9	24.1

Summary of bending test results of 22-layer design samples cured at 110 °C is given in Tables 9 and 10.

Table 9 : Bending test results for design samples

Sample Number	Width	Thickness	Area	Orientation	Failure Load	Ultimate Surface Strength	Maximum Deflection	Max outer surface Strain
	mm	mm	mm ²		N	MPa	mm	%
B1	15.8	4.1	64.6	[0,0,0,+45,0,-45,0,.....] _{11s}	235	219	21.7	1.96
B2	15.6	4.12	64.4	[0,0,0,+45,0,-45,0,.....] _{11s}	175	163	12.6	1.15
B3	15.7	4.37	68.6	[0,0,0,+45,0,-45,0,.....] _{11s}	134	111	5.83	0.562

Table 10: Flexural modulus values for design samples

Sample Number	Width	Thickness	Area	Orientation	Initial Flexural Modulus	Middle Flexural Modulus	Final Flexural Modulus	Average Flexural Modulus
	mm	mm	mm ²		GPa	GPa	GPa	GPa
B1	15.8	4.1	64.6	[0,0,0,+45,0,-45,0,.....] _{11s}	23	13	5.42	13.8
B2	15.6	4.12	64.4	[0,0,0,+45,0,-45,0,.....] _{11s}	21.6	11.4	4.08	12.4
B3	15.7	4.37	68.6	[0,0,0,+45,0,-45,0,.....] _{11s}	20.2	N/A	N/A	N/A

The ultimate failure loads, ultimate flexural strength, maximum deflection, maximum outer-surface strain and flexural modulus of all the unidirectional samples tested in three point bending are given in Figure 40 to Figure 44. Further discussion of these results is found in the Discussion section.

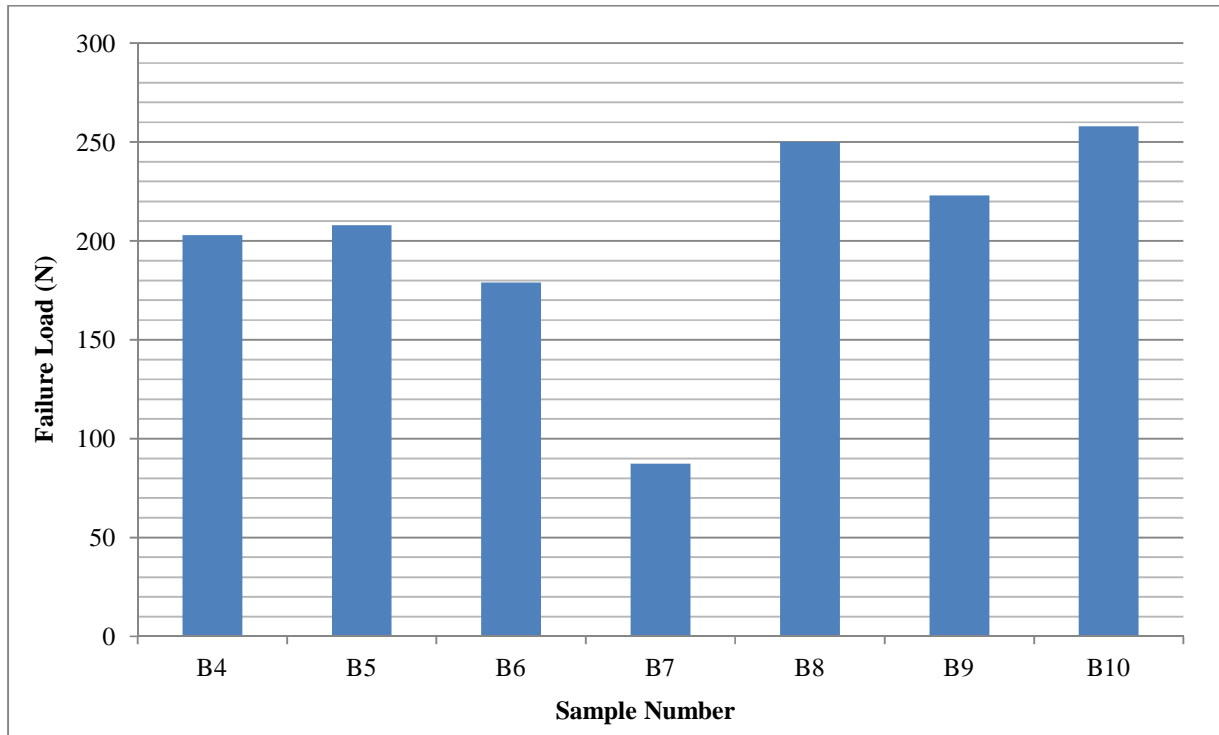


Figure 40: Bending failure loads of unidirectional samples

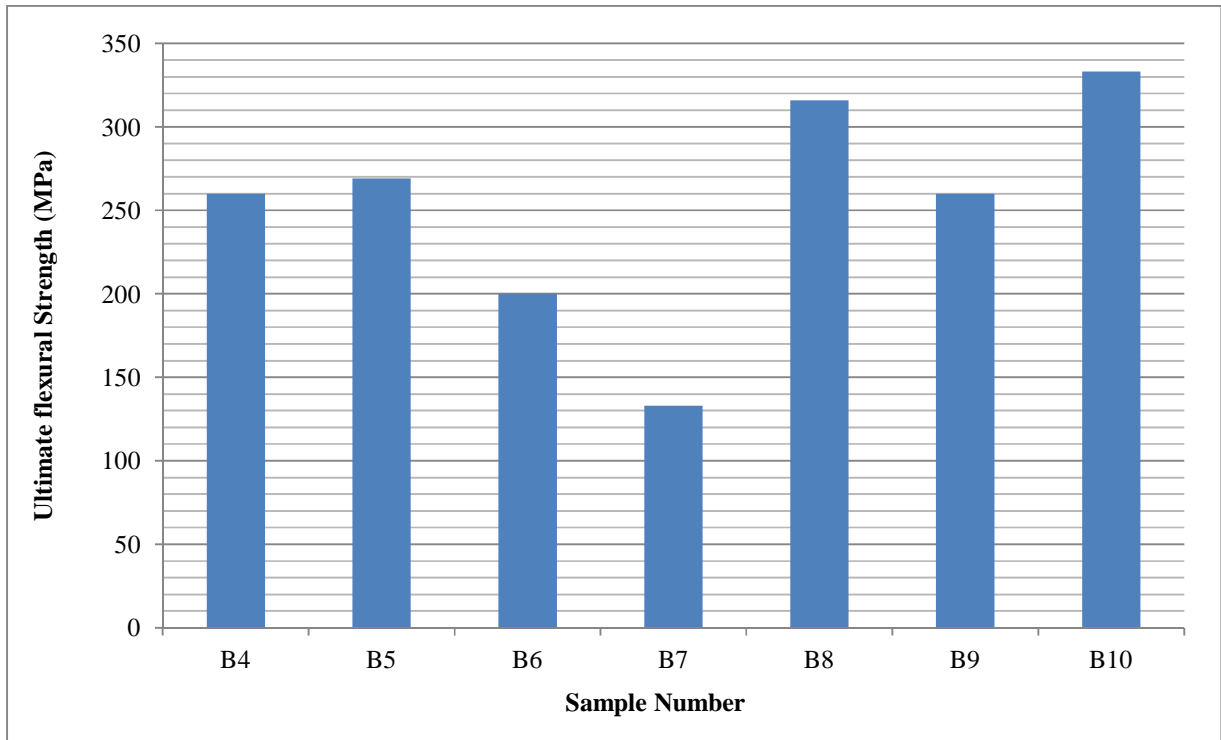


Figure 41: Ultimate flexural strength of unidirectional samples

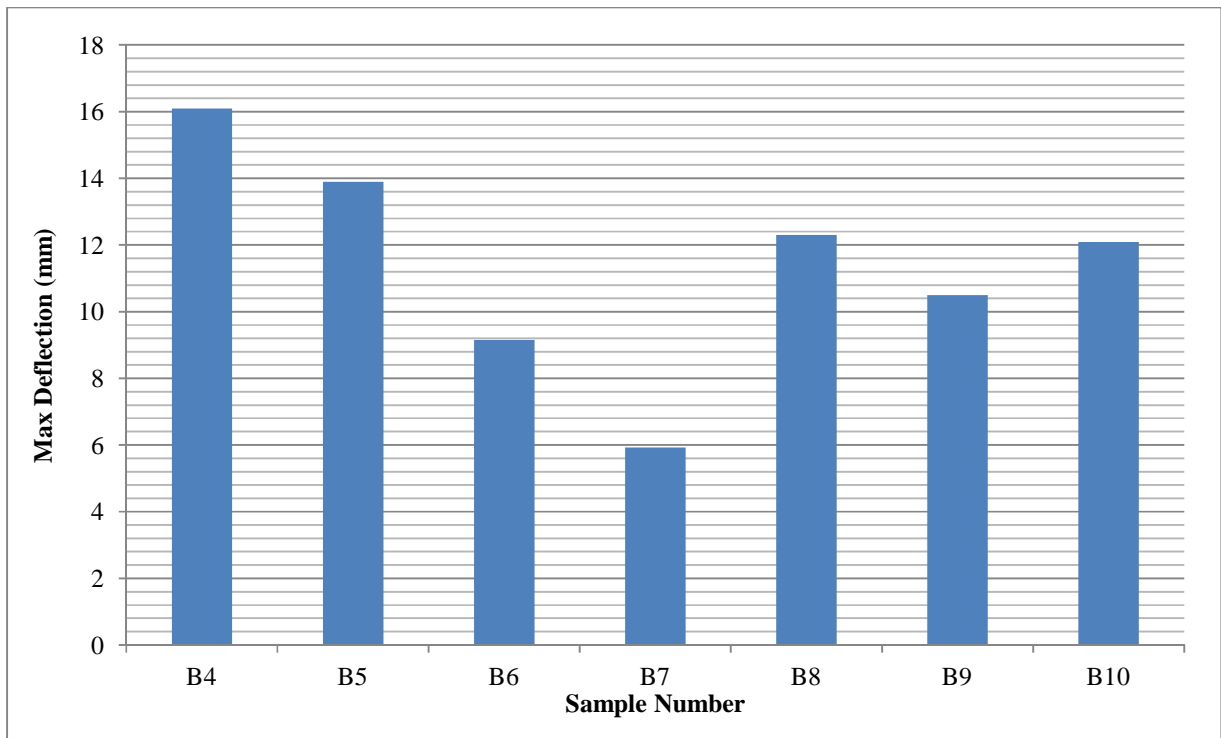


Figure 42: Maximum deflection of unidirectional samples

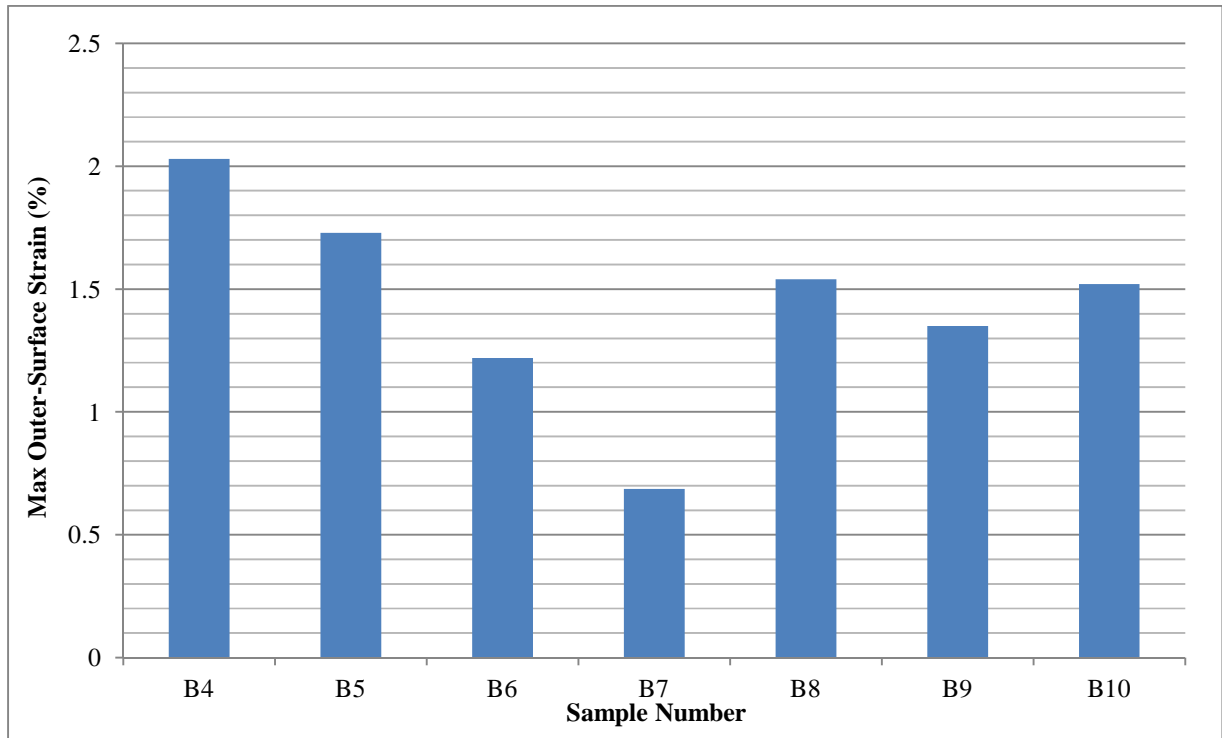


Figure 43: Maximum outer-surface strain of unidirectional samples

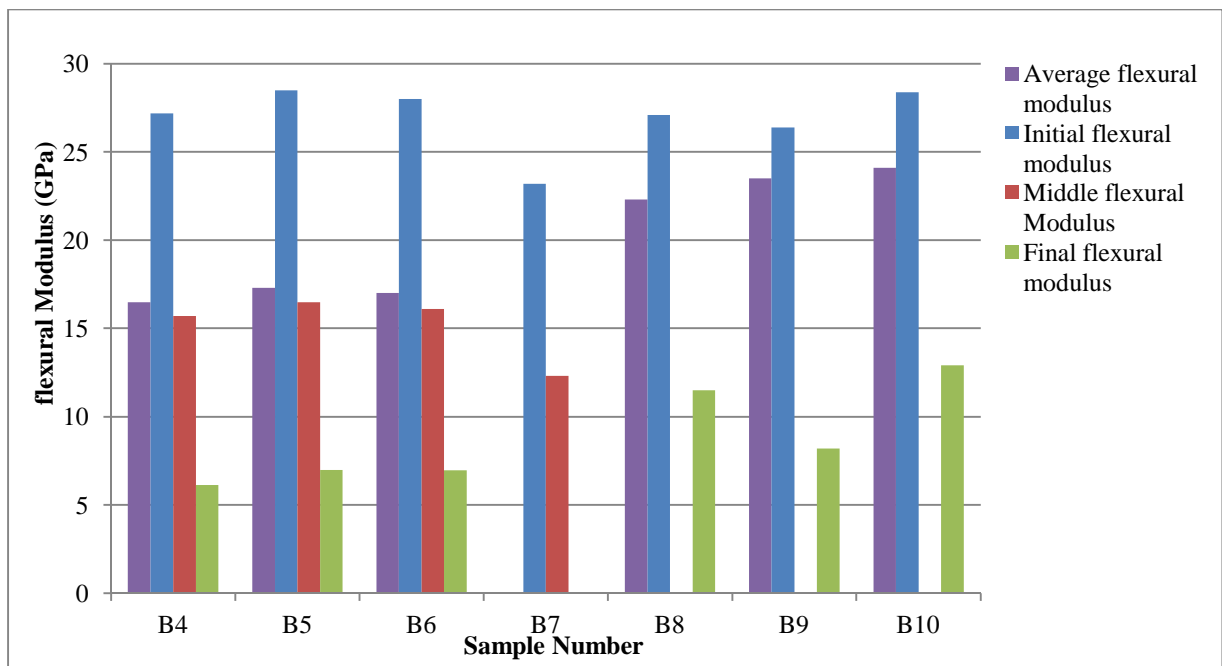


Figure 44: Flexural modulus of unidirectional sample

The ultimate failure loads, ultimate flexural strength, maximum deflection, maximum outer-surface strain and flexural modulus of the design samples tested in three point bending are given in Figure 45 to Figure 49. Further discussion of these results is found in the Discussion section.

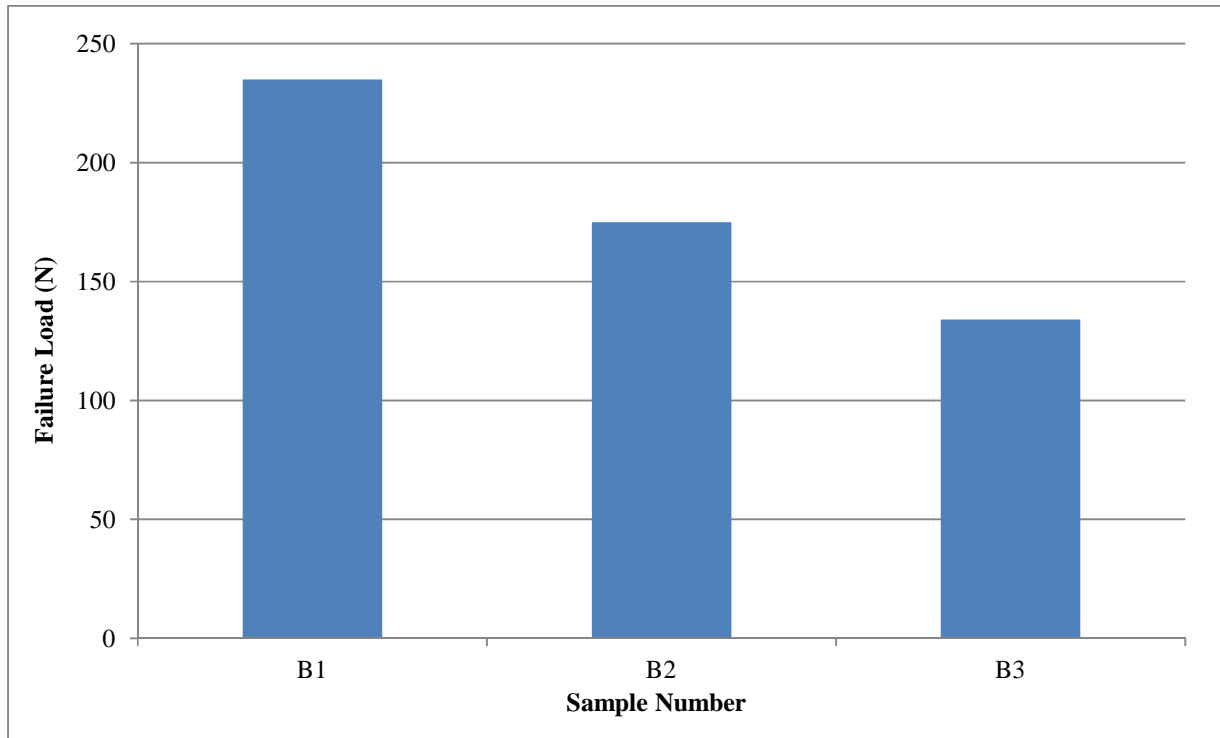


Figure 45: Bending failure loads of design samples

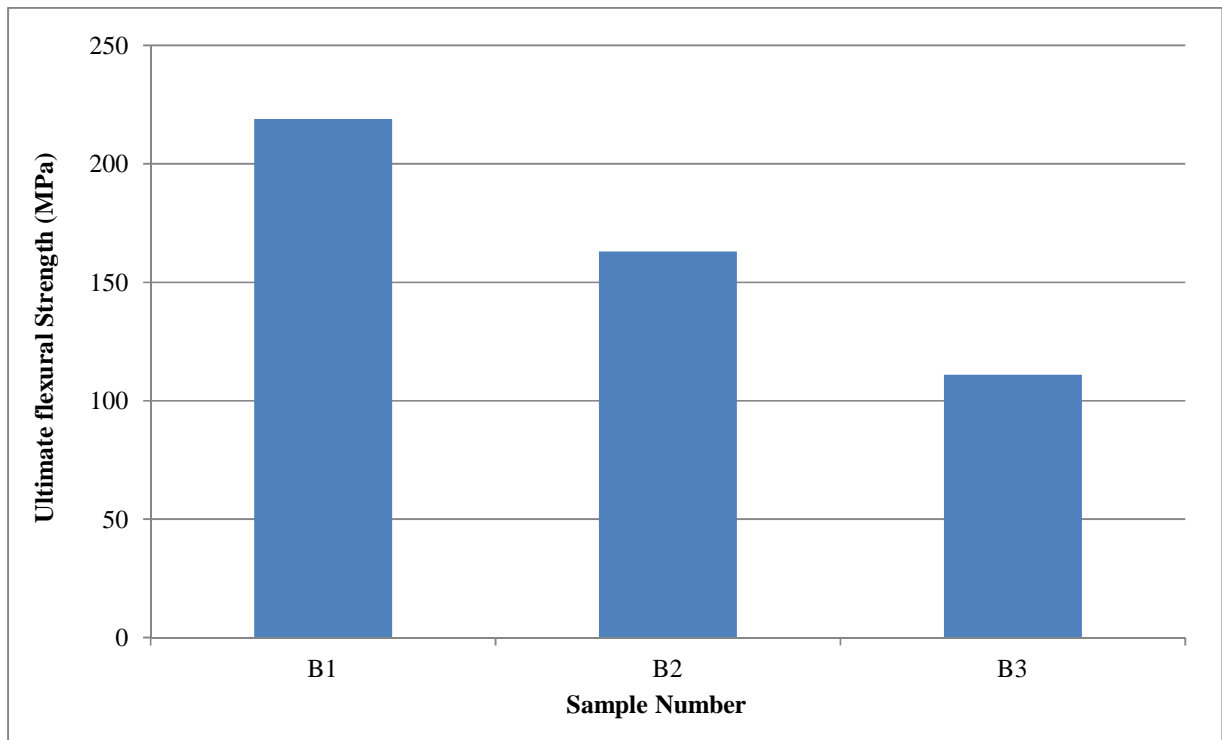


Figure 46: Ultimate flexural strength of design samples

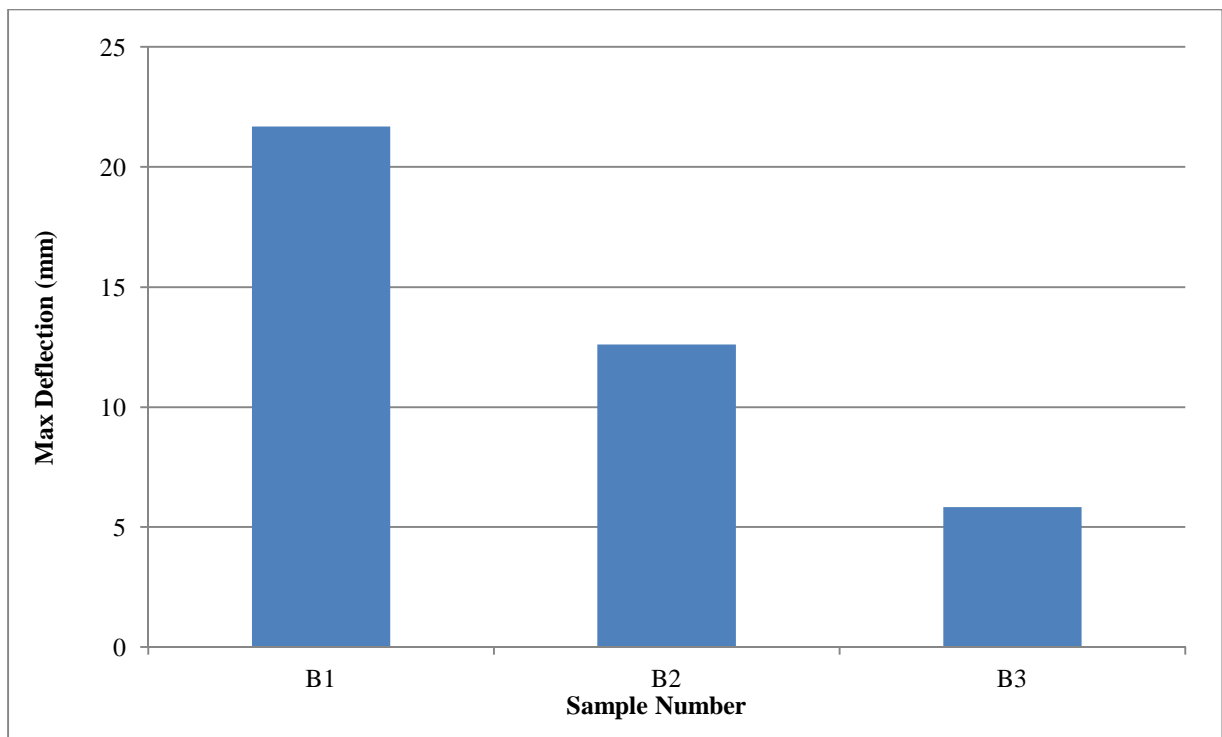


Figure 47: Maximum deflection of design samples

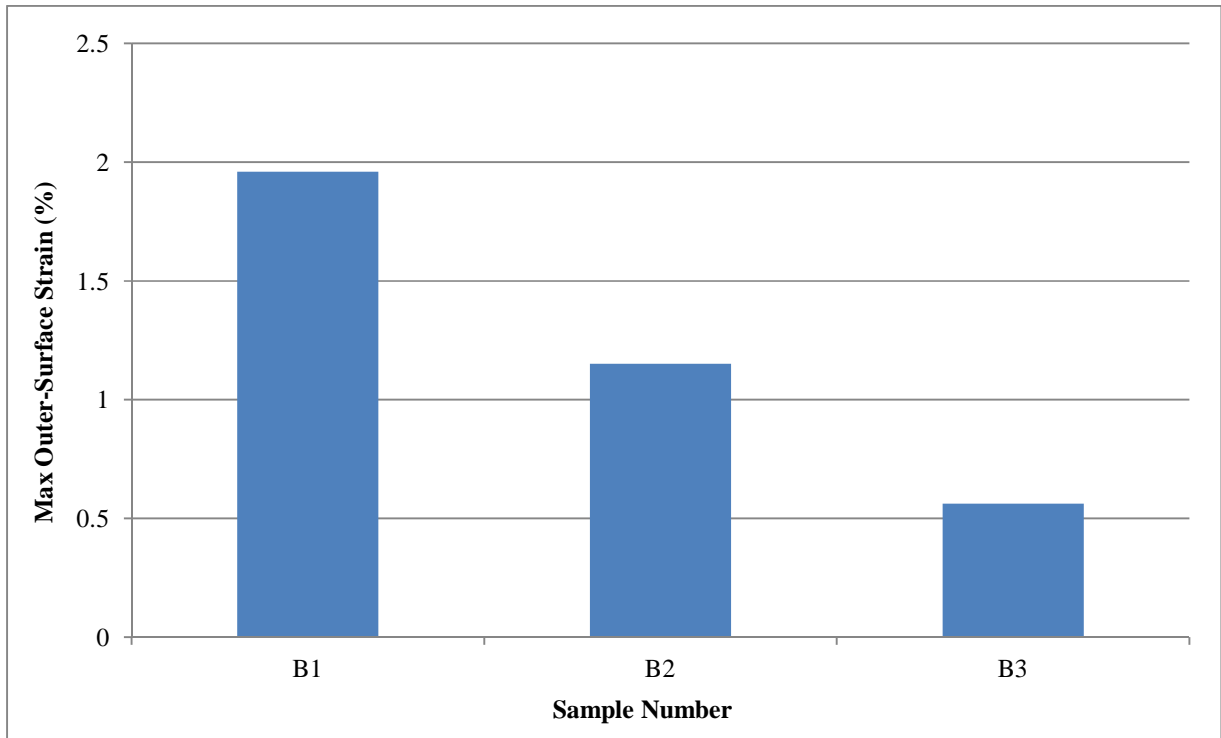


Figure 48: Maximum outer-surface strain of design samples

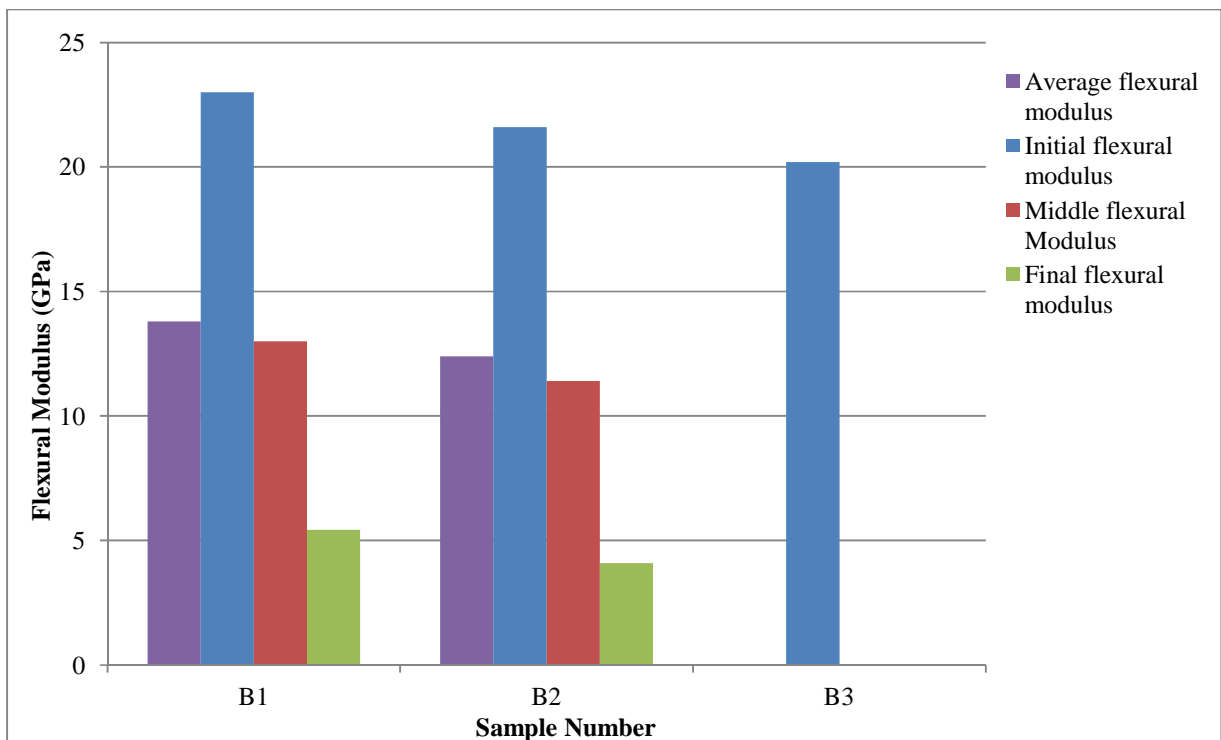


Figure 49: Flexural modulus of design sampl

Graphs showing the flexural behaviour of unidirectional samples B5 (cured at 110 °C) and B10 (cured at 150 °C) and design sample B1 are given in Figure 50 to Figure 53 in which force is plotted against deflection. Further discussion of these graphs is found in the Discussion section.

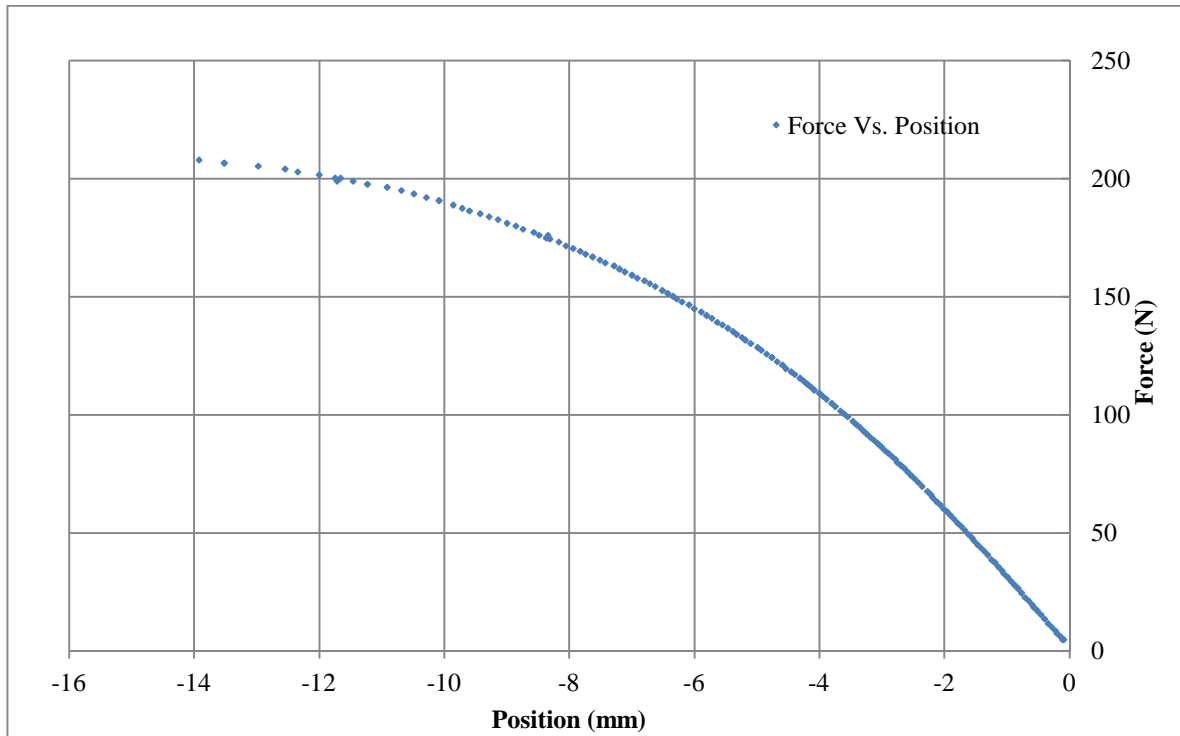


Figure 50: Flexural behaviour of unidirectional sample B5 cured at 110 °C

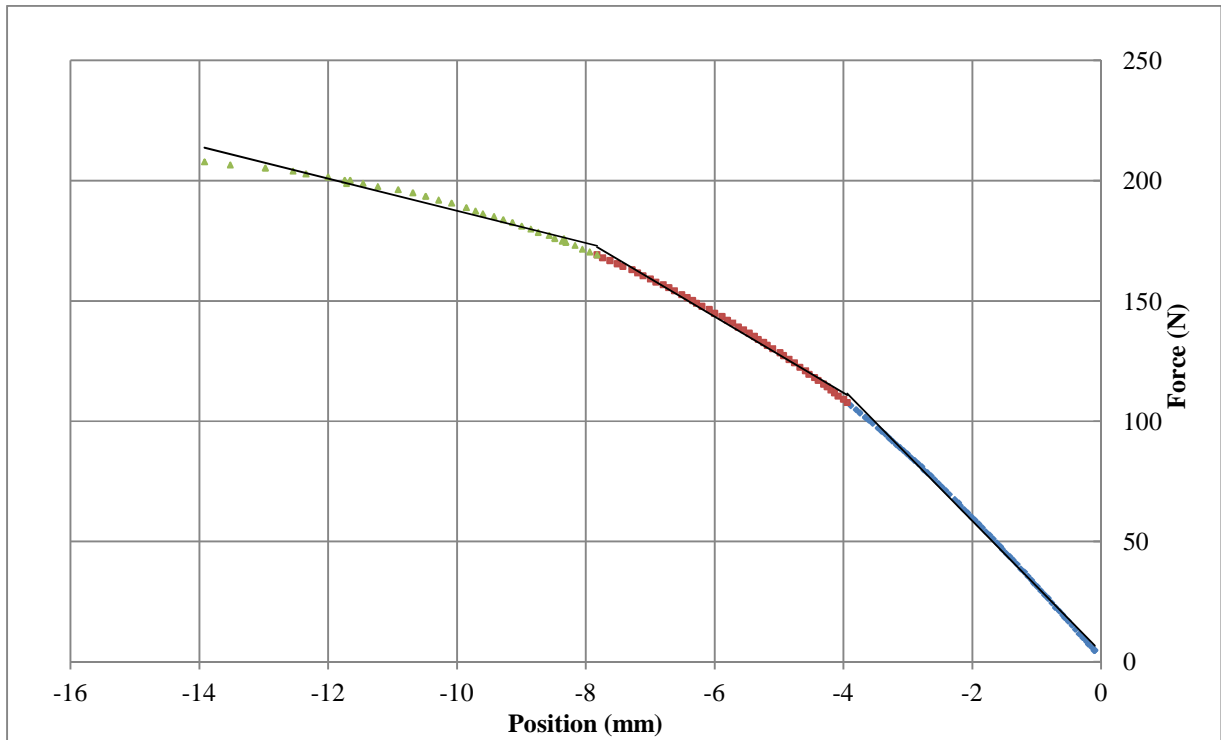


Figure 51: Regions of flexural behaviour of unidirectional sample B5 cured at 110 °C

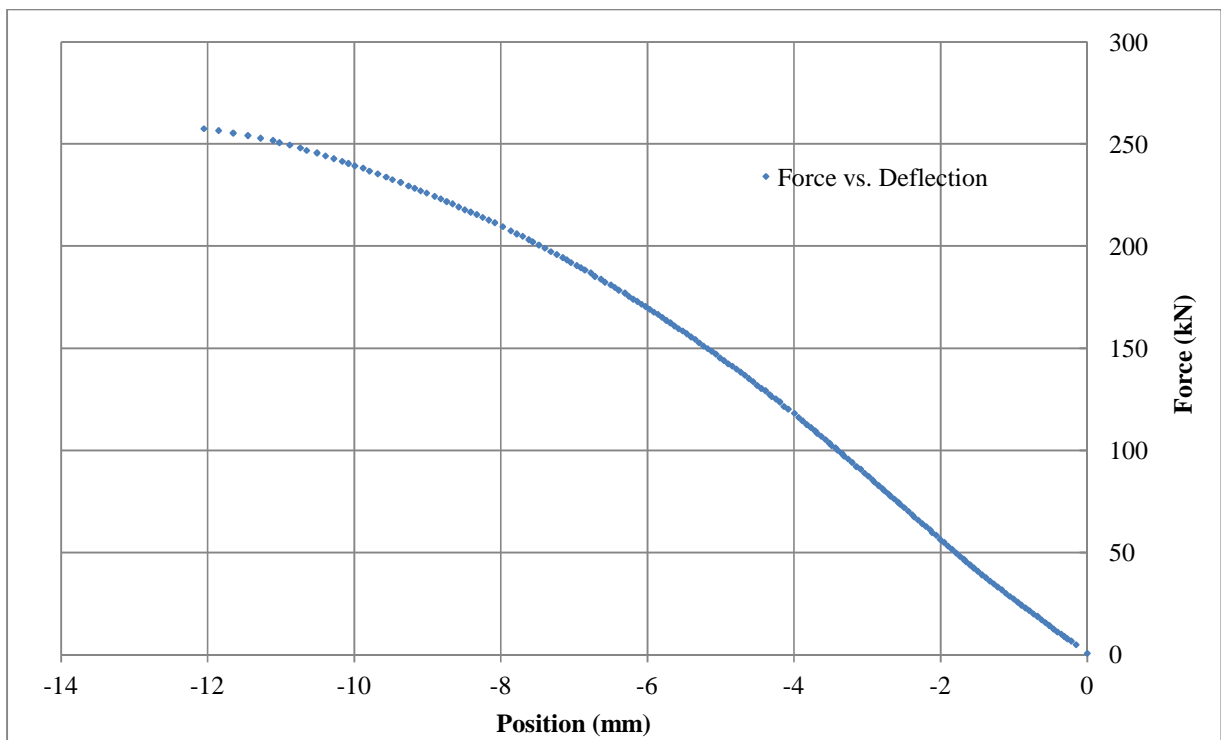


Figure 52: Flexural behaviour of unidirectional sample B10 cured at 150 °C

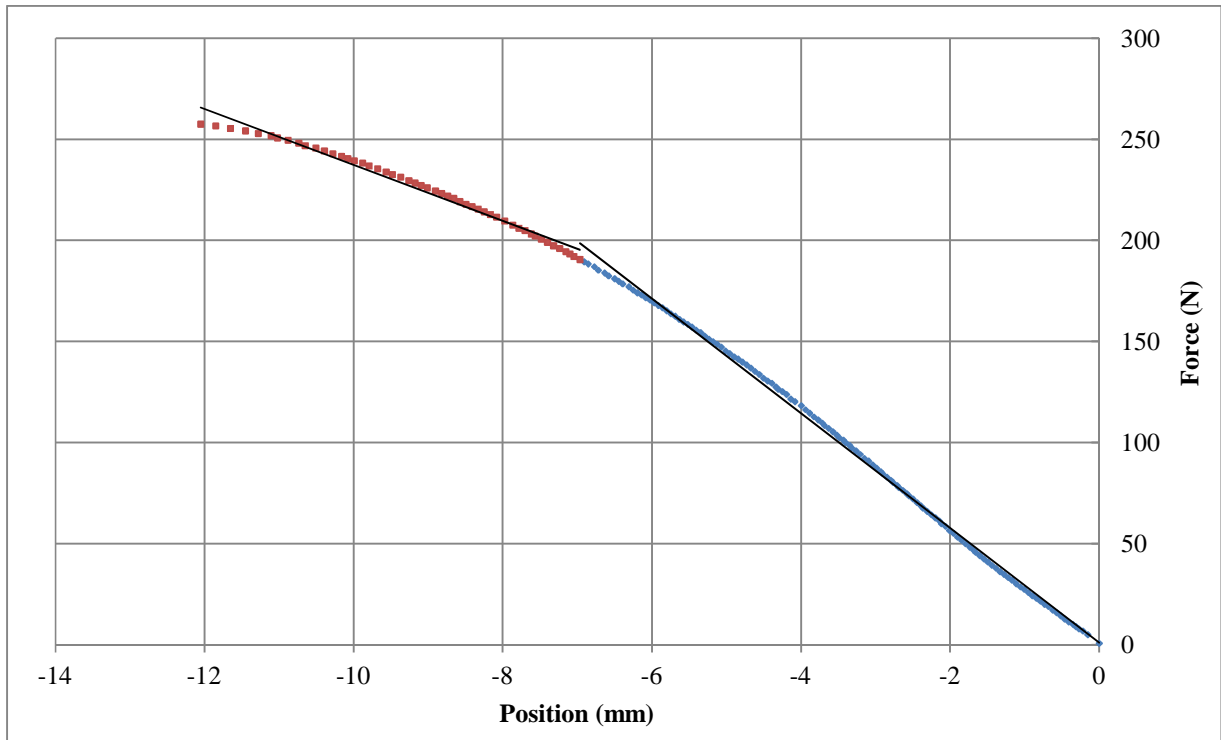


Figure 53: Regions of flexural behaviour of unidirectional sample B10 cured at 150 °C

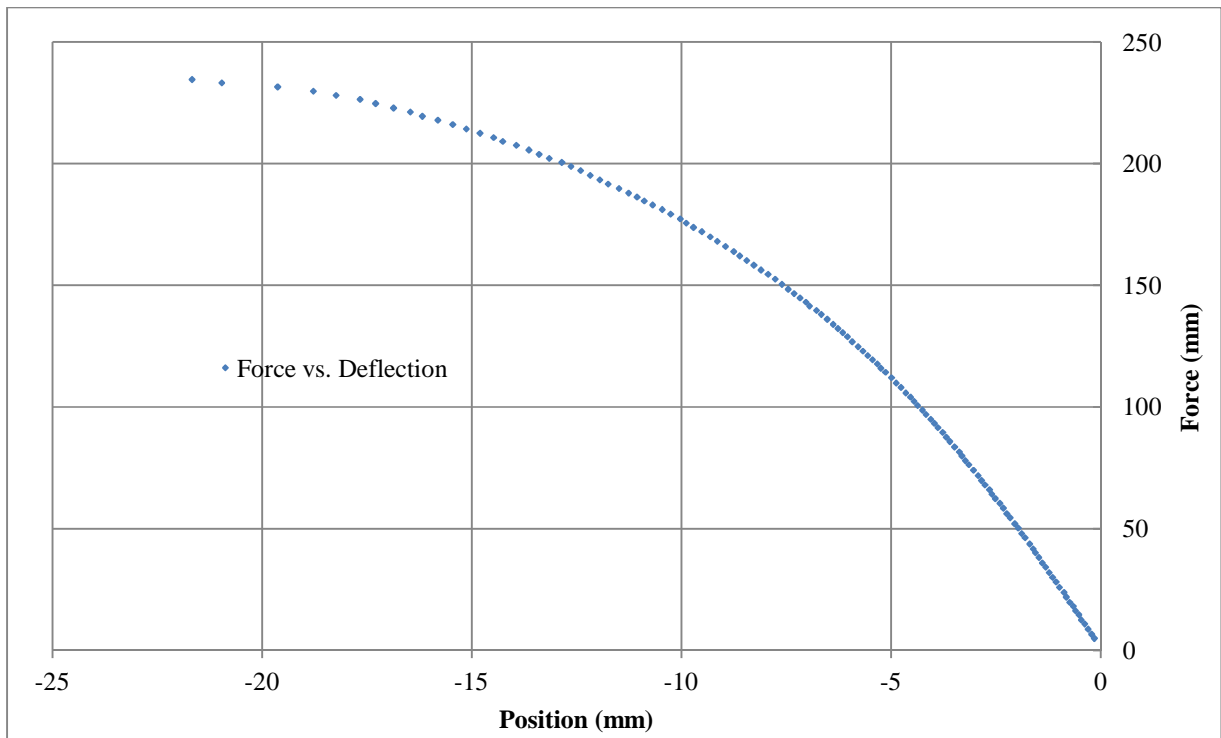


Figure 54: Flexural behaviour of design sample B1 cured at 110 °C

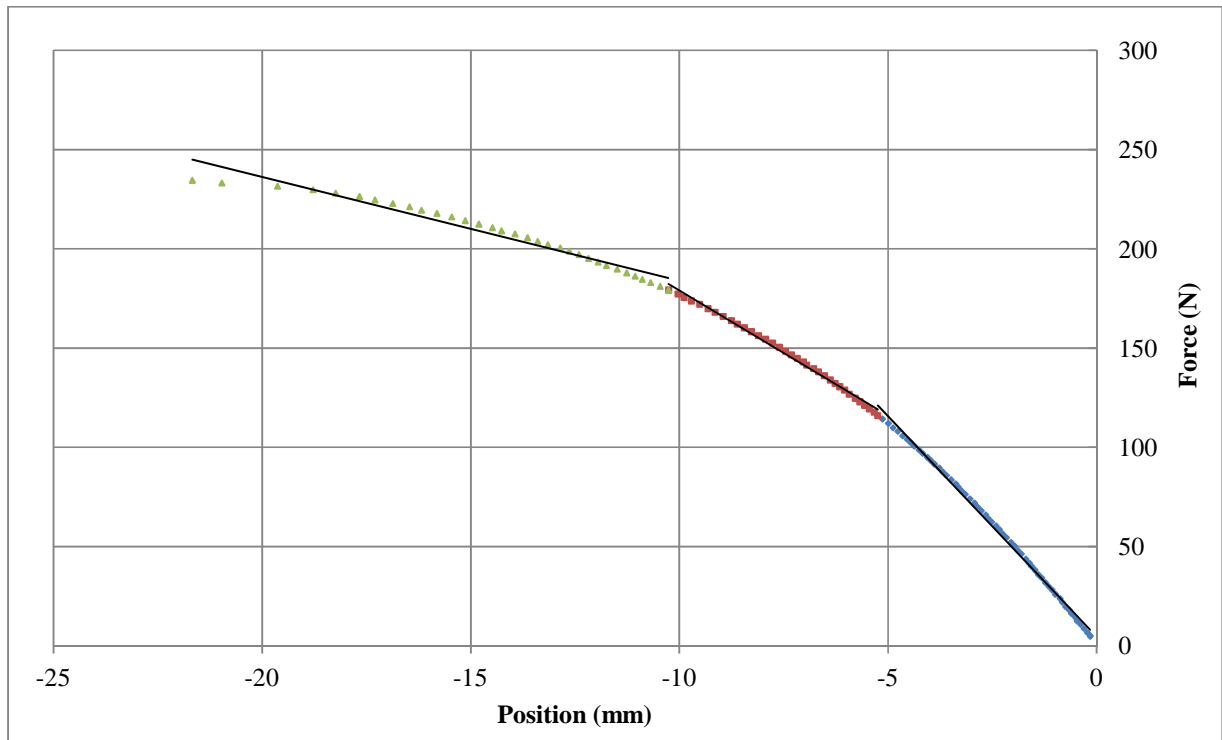


Figure 55: Regions of flexural behaviour of design sample B1 cured at 110 °C

7.3 Fatigue Test Results

Summary of fatigue test results of the four design samples is given in Table 11.

Table 11: Fatigue test results of design samples

Sample Number	Number of Layers	Orientation	Load	Percentage of Max Tensile Strength	Cycles to Failure
		°	kN	%	
F1	22	[0,0,0,+45,0,-45,0,.....] _{11s}	4.5	33	10,000,000*
F2	22	[0,0,0,+45,0,-45,0,.....] _{11s}	6.7	50	816,600
F3	22	[0,0,0,+45,0,-45,0,.....] _{11s}	8.7	65	3,800

*sample did not break

8. Discussion

8.1 Longitudinal Properties of Unidirectional Samples

Unidirectional samples cured at different temperatures and subjected to tensile loading in the longitudinal direction exhibited similarities in their tensile behaviour while showing differences in their ultimate tensile strength and failure strain values. Stress versus strain plots of samples T4 (cured at 110 °C) and T17 (cured at 150 °C) are quite representative of the tensile behaviour of all the tested unidirectional samples. The stress-strain curves begin as non-linear until a strain of about 0.2% and then become linear until the failure of the sample which happens at a strain of 1.0% to 1.5% depending on the sample and its curing temperature. This can be seen clearly in Figures 30 and 32. The linear section is the dominant part of the curve and can be used to find the value of the Young's modulus of the sample as shown in Figures 31 and 33.

The Young's modulus values of all unidirectional samples shown in Table 1 and compared in Figure 20 are consistent. Samples cured at 110 °C ranged in Young's modulus from 20.6 to 22.1 GPa (except for sample T7). Samples cured at 150 °C had Young's modulus values ranging from 21.6 to 25.9 GPa (except for sample T9). However 4 out of the 6 samples cured at 150 °C had a Young's modulus values between 25.3 and 25.9 GPa. Samples cured at an intermediate temperature exhibited Young's modulus values ranging from 21.9 to 22.6 GPa (except for one sample with a value of 25.2 GPa). These results, although not showing a great variation between samples cured at different temperatures, are quite logical as higher curing temperatures cause the epoxy matrix, and thus the whole composite, to have higher stiffness.

The values of ultimate tensile strength and failure strains are shown in Table 1 and compared in Figure 18 and 19. It can be seen that samples cured at 150 °C failed at slightly higher stresses and lower strains than samples cured at 110 °C; however, the samples cured at the intermediate temperature failed at higher stresses and strains than both. This seems inconsistent with previous results; nonetheless, it can be attributed to the manufacturing process. Samples cured at the intermediate temperature were put through a number of curing cycle ranging from 110 °C and 150 °C (thus the exact curing

temperature is unknown but it can be said to be between 110 °C and 150 °C). This meant that these samples had more time in the oven which is likely to have lead to enhanced consolidation and strengthening of the composite. In addition, these samples had larger cross sectional areas than the samples cured at 110 °C and 150 °C which is likely to have reduced the effect of impurities, voids and defects on the overall strength of the composite.

8.2 Transverse Properties of Unidirectional samples

The transverse behaviour of unidirectional samples cured at 110 °C and 150 °C is quite different as can be seen from stress versus strain curves for samples T22 and T18 shown in Figures 36 and 38. The sample cured at 110 °C exhibited two regions of linearity with significantly different slopes while the sample cured at 150 °C showed mostly a single linear behaviour. The matrix plays the dominant role in the transverse behaviour of a unidirectional composite which explains the previous results. Epoxy has higher and more linear stiffness behaviour when cured at higher temperatures thus the composite is stiffer in the transverse direction for the curing temperature of 150 °C.

The transverse modulus of the samples cured at the higher temperature can be found directly from the dominant linear portion of the stress vs. strain curve as shown in Figure 39. For the samples cured at the lower temperature the transverse modulus is an average of the two linear regions as shown in Figure 37. When compared to longitudinal properties, the transverse strength, failure strain, and modulus of samples cured at 150 °C are considerable higher than for those cured at 110 °C. The transverse tests give consistent results as can be seen from Table 2 and Figure 21 and 23 with the stiffer samples having transverse modulus values ranging from 4.28 to 5 GPa and the less stiffer samples ranging from 2.47 to 3.31 GPa.

8.3 Longitudinal Properties of Two-Directional Samples

In composites, addition of layers that are not in the direction of the axial load has the advantage of strengthening the composite material to better carry in-plane shear loads and torsional loads. Nevertheless, tow-directional composites are weaker and less stiff than their unidirectional counterparts in the axial direction. Table 5 and Table 6 together with Figures 24 and 29 serve to show this. Cross ply, quasi-isotropic, and design samples had

similar maximum strain values to those found in unidirectional samples, however, they had significantly lower ultimate strength and Young's modulus values. This means that two-directional samples are less stiffer than unidirectional samples and weaker when it comes to carrying axial loads. It would also mean that two-directional samples have lower flexural stiffness and strength when they are subjected to bending loads.

The tensile behaviour of design sample T13 can be seen from stress versus strain curves given in Figure 34 and 35. The tensile behaviour of sample T13 is not fundamentally different from unidirectional samples T4 and T17, however, the initial non-linear section is larger in sample T13 and extends to around 0.4% strain. This is due to the presence of layers oriented at plus and minus 45 degrees which decreases the axial stiffness and increases the elasticity of the composite.

8.4 Flexural Properties of Unidirectional Samples

The flexural behaviour of unidirectional samples cured at 110 °C and 150 °C can be illustrated by looking at the force versus deflection graphs of samples B5 (cured at 110 °C) and B10 (cured at 150 °C) shown in Figures 50 and 52. Flexural behaviour of both samples is non-linear, however, the sample cured at the higher temperature show higher linearity than the one cured at the lower temperature. This is illustrated further in Figures 51 and 53 where the force versus deflection curves are divided into regions of linearity. The curve for sample B5 shows a highly non-linear behaviour, but it can be approximately divided into an initial, middle, and final regions of linearity. In comparison, the curve for sample B10 is much more linear and can be approximately divided into a dominant initial and a less dominate final regions of linearity. This behaviour can be attributed to the role of the matrix as epoxy is stiffer and act more linearly when cured at higher temperatures.

The previously observed behaviour can be seen more clearly when looking at Table 8 and Figure 44. All of the seven samples have similar initial flexural modulus ranging from 26.4 to 28.5 GPa (except for sample B7). However, the flexural stiffness of samples B4 to B7 starts declining after this initial region, goes into a middle region in the range of 15.7 to 16.5 GPa, and finally into a final region in the range of 6.12 to 6.98 GPa (except for sample B7). In contrast, samples B8 to B10 have a much larger initial linear region

leading into a final smaller region of a flexural stiffness ranging from 8.19 to 12.9 GPa. The average flexural modulus of samples cured at 150 °C ranges from 22.3 to 24.1 GPa while for the samples cured at 110 °C ranges from 16.5 to 17.3 GPa.

This flexural behaviour can be further seen when looking at Table 7 and Figures 40 to 43. It is clear that the samples cured at 150°C are stiffer than those cured at 110°C as they have higher ultimate flexural strength and lower maximum outer surface strain. The test results are quite consistent for samples B8 to B10 (the stiffer samples) and mostly consistent for samples B4 to B7 except for sample B7 which had an early failure.

8.5 Flexural Properties of Two-Directional Samples

The flexural behaviour of two-dimensional design samples can be seen from the force versus deflection curve of sample B1 given in Figures 54 and 55. The behaviour of sample B1 is very similar to the behaviour of unidirectional sample B5 in showing three different regions of linearity. This is no surprise as both samples are cured at 110 °C thus having similar matrix properties. However, the average flexural modulus for B1 is 13.8 GPa compared to 17.3 for B5. This is also no surprise as the presence of layers oriented at plus and minus 45 degrees lowers the flexural stiffness of the design composite.

Results in Table 10, compared Figure 49, show consistency in the values of the flexural modulus among the three tested samples (B1 to B3). The initial flexural modulus ranged from 20.2 to 23 GPa, middle modulus from 11.4 to 13 GPa, and final modulus from 4.08 to 5.42 GPa (except for sample B3 which had no middle and final regions because of early failure). Table 9 and Figures 45 and 49 can be used to compare the performance of the three samples which failed at considerably different loads and deflections. The premature failure of samples is indicative of faulty manufacturing and confirms the previous notion that the manufacturing equipment and process were far from ideal.

8.6 Flax-Epoxy Composites for Bone Fixation Plates

Results from previous tests can be used to determine the mechanical suitability of this flax-epoxy composite material for making bone fixation plates. Unidirectional samples tested in the longitudinal direction yielded Young's Modulus values ranging from 20.6 to 25.9 GPa (which largely depended on the curing temperature of the sample). On the one

hand, this range can be considered absolutely ideal for orthopaedic applications, as the average Young's modulus for cortical bone is 20 GPa. On the other hand, it can be a limiting factor as the use of two-directional configurations will cause the value of the Young's modulus to drop below that of bone which compromises the suitability of the material for the intended application. For example, from Table 5, the Young's modulus can be as low 8 GPa when the quasi-isotropic [0,+45,90,-45] configuration is used.

A low Young's modulus also means a low flexural modulus which is quite problematic. Bending test of samples cured at 110 °C and 150 °C revealed initial flexural modulus (secant flexural modulus) values ranging from 26.4 to 28.5. However, the average flexural modulus of 110 °C samples was around 17 GPa while that of 150 °C samples was around 23 GPa. The curing temperature becomes quite important when flexion is concerned as higher curing temperatures increase the stiffness of the matrix, and thus the whole composite, and enhances flexural linearity by making the initial flexural region the largest and most dominant region of the flexural curve. Results demonstrate that 110 °C samples deflected by as much as 16 mm under a load of 200 N while 150 °C samples by as much as 12 mm under a load of 250 N. Samples cured at the higher temperature obviously performed better than those cured at the lower temperature, however, their level of deflection under such small loads was still too high for a bone fixation plate.

The design configuration in which approximately 65% of plies were oriented in the zero direction and 35% in the plus and minus 45 direction was chosen as an attempt to strengthen the implant for in-plan shear loads and torsional loads while maintaining a Young's modulus close to that of the bone. Tensile testing of design samples (which had dimensions identical to those of metallic implants) revealed a Young's modulus of 15 GPa, ultimate tensile strength of 200 MPa (Failure loads of around 13.6 kN), and failure strain of 1.2%. These values are quite satisfactory as far as axial loading is concerned since the tensile strength is high enough to carry the body load (which is about 2.5 to 3 kN), and the Young's modulus is close enough to that of the bone to allow for stress transfer to the fracture location and thus induce a healthy healing process.

The difficulty arises when flexion is taken into account. Bending test of the design samples yielded initial flexural modulus values in the range of 20 to 23 GPa and much lower average flexural modulus values of 13.8 GPa for sample B1 and 12.4 GPa for sample B2 (Sample B3 failed prematurely and never passed the initial region). This meant that sample B1 deflected by 21.7 mm under a load of 235 N and sample B2 by 12.6 mm under a load of 175 N. These low average flexural modulus values can partially be attributed to the fact that the design samples were cured at 110 °C. Flexural testing had not yet been performed when the design configuration was chosen and the lower curing temperature was thought to be beneficial in providing more flexibility in the axial direction. However, even at a higher curing temperature, the design samples would still be unsatisfactory since its flexural stiffness is weakened by the presence of plies oriented at plus and minus 45 degrees. Besides, even if the design samples were unidirectional, it is unlikely that they would be stiff enough for holding the two sides of a fractured bone sufficiently immobilized when subjected to bending.

8.7 Optimization of Plate Design

The limitations arising from the high flexural flexibility of the flax-epoxy composite can be overcome by manipulating design parameter such as the number of plies, orientation of plies, cross sectional area and the curing temperature of the composite. If this proves unsatisfactory or impractical, the desired flexural stiffness can be achieved by reinforcing the outer surfaces of the flax-epoxy composite with plies of carbon or other stiffer fibres.

From the previous investigation it can be seen that a high curing temperature is beneficial for a bone fixation implant since it considerably increase both the transverse and flexural stiffness and strength of the implant. The use of a unidirectional design is necessary to maximize the flexural stiffness if carbon fibres or other stiffer fibres are not to be introduced into the implant. The low flexural stiffness of the flax-epoxy composite compared to other materials that have been traditionally used for bone fixation plates, such as titanium or Carbon-Carbon composites, can be compensated for by increasing the cross sectional area of the implant.

This can be best achieved by increasing the thickness (i.e. the number of layers) of the flax-epoxy implant. In beam bending theory, the maximum deflection of a beam with a rectangular cross-sectional area is inversely proportional to the cube of its thickness. This relation can be used to find the necessary thickness of the flax-epoxy implant that would have a similar bending deflection to what is found in titanium or C-C implants. A simple calculation shows that a flax-epoxy implant with a thickness of 6.5 mm would have the same maximum deflection as a titanium implant 4 mm thick given that all other dimensions are equal and the two implant are subjected to the same load. A similar calculation shows that a flax-epoxy implant with a thickness of 5.5 would have the same maximum deflection as a C-C implant 4 mm thick given that all other dimensions are equal. A Summary of the flax-epoxy implant design parameter optimized to match the performance of traditional materials is given in Table 12. A bar chart comparing the Young's Modulus values of traditional implant material and flax-epoxy composites is given in Figure 56.

Table 12: Summary of optimized design parameters

Material to be Matched	Width	Thickness	Number of Layers	Orientation	Curing Temperature
	mm	mm		°	°C
Stainless Steel	15	8.0	44	UD	150
Titanium	15	6.5	36	UD	150
C-C	15	5.5	30	UD	150

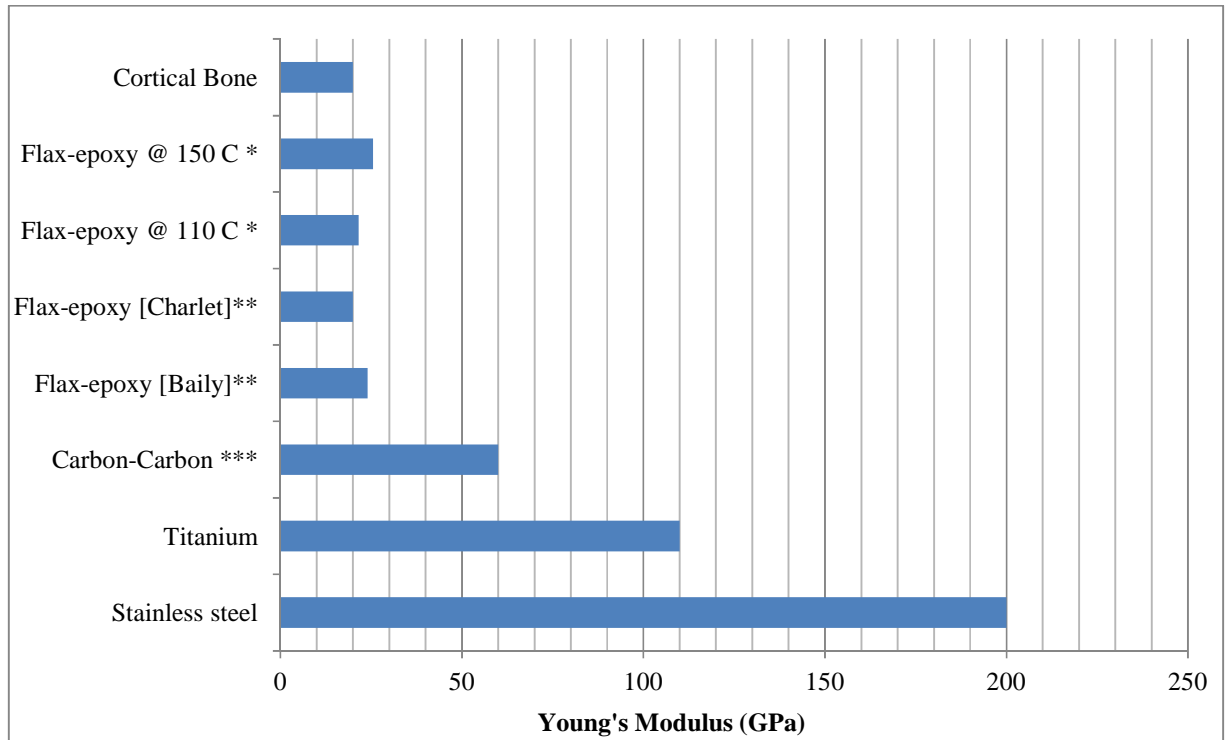


Figure 56: Comparison of Young's modulus values of different materials

* Flax-epoxy composite with 60% fibre volume

** Flax-epoxy composite with 40% fibre volume. Curing temperature unreported.

*** Most common value for C-C composites

9. Conclusions

In this research work, a flax-epoxy prepreg was experimentally investigated as a potential composite material for making orthopaedic implants in general, and bone fixation plates in particular. The work involved manufacturing, mechanical testing, data analysis, and designing and optimizing of potential bone fixation implants. Overall, the material was found suitable for bone fixation plates if designed correctly or combined with other types of fibre reinforcement.

The manufacturing process was a limiting factor in terms of both the quality and quantity of samples that could be produced. This was confirmed by the premature failure of a number of samples in both tensile and bending tests and the superiority of samples cured at multiple stages and had larger cross sectional areas over those cured at a single cure cycle and had smaller cross sectional areas. In addition, testing of a larger number and variety of samples would have been possible had better manufacturing facilities been available.

Mechanical testing yielded largely consistent results despite the premature failure of a number of samples as mentioned above. Through tensile and flexural testing it was possible to do the mechanical characterization of the composite material and find its Young's modulus, transverse modulus, shear modulus, and Poisson's ratio. This information is quite useful for researchers and designers looking to use flax-epoxy composites whether in orthopaedics or other fields.

The test results coincided quite well with data found in the literature and listed in the literature review. Results also showed the influence of the curing temperature on the overall stiffness of the matrix. Young's modulus values for unidirectional samples ranged from 20 to 25 GPa, ultimate strength from 275 to 350 MPa, and maximum strain from 1.10 to 1.60 percent.

The flax-epoxy prepreg has a Young's modulus almost identical to that of bone while at the same time posing high strength which makes it a suitable material for orthopaedic applications. Therefore, flax-epoxy composite can be an ideal candidate to make joint

replacements or bone fixation plates. The only challenge is that with low stiffness comes large flexural deflections. This is not permissible for bone fixation plates which are supposed to maintain the two sides of the fracture bone immobilized. This challenge can be overcome by manipulating the design parameters (width, thickness, number of plies, orientation of plies) so that flexural deflection does not exceed what is acceptable for this application. Another option would be to reinforce the flax-epoxy composite with stiffer fibres such as carbon fibres.

If the flax-epoxy composite is not to be reinforced with other fibres then it is necessary to make the bone fixation implant out of a unidirectional composite in order to maximize its flexural stiffness. However, this in itself is insufficient to prevent excessive flexural deflection. The low stiffness of the flax-epoxy composite has to be compensated for by increasing the cross sectional area of the implant, especially its thickness i.e. number of plies. This is not a problem from a weight point of view since the material is very light; however, increased cross sectional area may create difficulties from a surgical point of view. This needs to be further investigated.

Beam bending theory can be used to find what thicknesses of the flax-epoxy composite would be necessary to match the flexural strength of metallic or carbon implants given that all other dimensions (width and length) are equal. A simple calculations shows that to have a maximum bending deflection similar to that of a stainless steel implant, a unidirectional flax-epoxy implant must be 8 mm thick, to match a titanium implant, it must be 6.5 mm thick, and to match a carbon-carbon implant, it must be 5.5 mm thick.

These theoretical calculation and estimation are yet to be proven in experiment or numerical simulation. Building on the results of this work, the following future work is recommended:

- Manufacturing unidirectional samples of thicknesses ranging from 5.5 to 6.5 mm and testing them in tension and flexion.
- Manufacturing unidirectional samples 4 mm in thickness reinforced with carbon fibres and testing them in tension and flexion.

- Subjecting satisfactory designs to compression testing since compression is the main type of stress which an implant would be subjected to in the human body.
- Subjecting satisfactory designs to torsional testing to decide whether an implant made of a unidirectional composite is capable of resisting in-plane shear and torsional loads. If not, it would be necessary to come up with two-dimensional designs.
- Manufacturing design implants with screw holes in them and subjecting them to tension, flexural, compression and torsional testing. This is absolutely necessary to determine whether the design is satisfactory since the presence of holes significantly weakens the implant.
- Studying the suitability of the flax-epoxy composite for making artificial joint replacements and synthetic bones.

10. References

- [1] A. S. Singha and Vijay Kumar Thakur, "Flax as potential fiber for reinforcement in composites," in *Green Composites: Properties, Design and Life Cycle Assessment*, Francois Willems and Pieter Moens, Eds. New York: Nova Science Publishers, Inc., 2010, ch. 2, pp. 31-52.
- [2] A. S. Singha and V. K. Thakur, "Synthesis and characterization of Short Saccharum Cilliare fiber reinforced green composites," *International Journal of Plastic Technology*, vol. 11, pp. 835-851, 2007.
- [3] G. Romhany, J. Karger-Kocsis, and T. Czigany, "Tensile fracture and failure behaviour of technical flax fibres," *Journal of Applied Polymer Science*, vol. 90, pp. 3638-3645, 2003.
- [4] Mustafa Aslan, Gary Chinga-Carrasco, Bent F. Sorensen, and Bo Madsen, "Strength variability of single flax fibres," *Journal of Material Science*, vol. 46, pp. 6344-6354, 2011.
- [5] Karine Charlet, Jean Paul Jernot, Moussa Gomina, Laurent Bizet, and Joel Breard, "Mechanical properties of flax fibres and of the derived unidirectional composites," *Journal of Composite Materials*, vol. 44, pp. 2887-2896, 2010.
- [6] A. S. Singha, B. S. Kaith, and S. Kumar, "Evaluation of physical and chemical properties of FAS-KPS induced graft co-polymerization of binary vinyl monomer mixtures onto mercerized flax," *International Journal of Chemical Sciences*, vol. 2, pp. 472-482, 2004.
- [7] J. Anderson and R. Joffe, "Estimation of the tensile strength of an oriented flax fibre-reinforced polymer composite," *Composites: Part A*, vol. 42, pp. 1229-1235, 2011.

- [8] A. K. Mohanty, M. Misra, and G. Hinrichsen, "Biofibres, biodegradable polymers and biocomposites: An overview," *Macromolecular Materials and Engineering*, vol. 276-277, pp. 1-24, 2000.
- [9] C. Baley, "Analysis of the flax fibres tensile behaviour and analysis of the tensile stiffness increase," *Composites Part A*, vol. 33, pp. 939-948, 2002.
- [10] C. Baley and B. Lamy, "Stiffness prediction of flax fibres-epoxy composite materials," *Journal of Material Science Letters*, vol. 19, pp. 979-980, 2000.
- [11] A. K. Mohanty, M. Misra, and L. T. Drzal, "Surface modifications of natural fibers and performance of the resulting biocomposites: An overview," *Composite Interfaces*, vol. 8, pp. 313-343, 2001.
- [12] C. Baley, "Influence of kink bands on the tensile strength of flax fibres," *Journal of Material Science*, vol. 39, pp. 331-334, 2004.
- [13] R. M. Rowell, J. S. Han, and J. S. Rowell, "Characterization and factors affecting fibre properties," *Natural Polymers and Agrofibres Composites*, pp. 115-134, 2000.
- [14] M. Hugues et al., "An investigation into the effects of micro-compressive defects on interphase behaviour in hemp-epoxy composites using half-fringe photoelasticity," *Composite Interface*, vol. 7, pp. 13-29, 2000.
- [15] R. Karani, M. Krishnan, and R. Narayan, "Biofiber-reinforced polypropylene composites," *Polymer Engineering and Science*, vol. 7, pp. 476-483, 1997.
- [16] S. Sapiaha, J. F. Pupo, and H. P. Schreiber, "Thermal degradation of cellulose-containing composites during processing," *Journal of Applied Polymer Science*, vol. 37, pp. 233-240, 1989.
- [17] T. Stuart et al., "Structural biocomposites from flax—Part I: Effect of bio-technical fibre modification on composite properties," *Composites Part A*, vol. 37, pp. 393-404, 2006.

- [18] C. Baley, Y. Perrot, F. Busnel, H. Guezenoc, and P. Davies, "Transverse tensile behaviour of unidirectional plies reinforced with flax fibres," *Material Letters*, vol. 60, pp. 2984-2987, 2006.
- [19] J. Van Raemdonch, J. Van Acker, N. Defoirdt, and H. McKee, "Epoxy/Flax fiber prepregs: properties and applications," *SAMPE Journal*, vol. 44, pp. 6-12, 2008.
- [20] Francois Vanfleteren, "Flax-Epoxy prepregs leading the race," *JEC Composites Magazine*, no. 37, pp. 44-45, December 2007.
- [21] L. Reclaru, R. Lerf, P. Y. Eschler, and J. M. Meyer, "Corrosion behaviour of a welded stainless-steel orthopaedic implant," *Biomaterials*, vol. 22, pp. 269-279, 2001.
- [22] K. H. Kramer, "Implants for surgery - a survey on metallic materials," *Materials for Medical Engineering EUROMAT 99*, vol. 2, pp. 9-29, 1999.
- [23] S. Ramakrishna, J. Mayer, E. Wintermantel, and K. W. Leong, "Biomedical applications of polymer-composite based materials: a review," *Composites Science and Technology*, vol. 61, pp. 1189-1224, 2001.
- [24] S. L. Evans and P. J. Gregson, "Composite technology in load-bearing orthopaedic implants," *Biomaterials*, vol. 19, pp. 1329-1342.
- [25] J. Chlopek and G. Kmita, "Non-metallic composite materials for bone surgery," *Engineering Transactions*, vol. 51, no. 2-3, pp. 307-323, 2003.
- [26] L. L. Hench, "Biomaterials: a forecast for the future," *Biomaterials*, vol. 19, pp. 1419-1423, 1998.
- [27] J. C. Middleton and A. J. Tipton, "Synthetic biodegradable polymers as orthopaedic devices," *Biomaterials*, vol. 21, pp. 2335-2346.
- [28] K. J.L. Burg, S. Porter, and J. F. Kellam, "Biomaterial developments for bone tissue

- engineering," *Biomaterials*, vol. 21, pp. 2347-2359, 2000.
- [29] M. Blazewicz, "Carbon grafts produced from polyacryloniryle in treatment of soft tissues," *Polymers in Medicine* , vol. 1-2, pp. 33-39, 2001.
- [30] M. Blazewicz, "Carbon materials in the treatment of soft and hard tissue injuries," *European Cells and Materials*, vol. 2, pp. 21-29, 2001.
- [31] W. Suchanek, M. Yashima, M. Kakihana, and M. Yoshimura, "Processing and mechanical properties of hydroxyapatite reinforced with hydroxyapatite whiskers," *Biomaterials*, vol. 17, pp. 1715-1723, 1996.
- [32] J. Chlopek et al., "Composite stems for dog's hip joint endoprosthesis," *Engineering of Biomaterials*, vol. 10, pp. 8-17, 2000.
- [33] J. Chlopek et al., "Carbon and polymer composites in bone surgery," *Materials for Medical Engineering EUROMAT 99*, vol. 2, pp. 103-109, 1999.
- [34] A. Stoch, A. Brozek, and A. Adamczyk, "Elctrocrystallization of hydroxyapatite coatings on carbon biomaterials," *Engineering of Biomaterials*, vol. 17-19, pp. 19-20, 2001.
- [35] D. Chandramohan and K. Marimuthu, "Characterization of natural fibers and their application in bone grafting substitutes," *Acta of Bioengineering and Biomechanics*, vol. 13, pp. 77-84, 2011.
- [36] D. Chandramohan and K. Marimuthu, "Natural fiber particle reinforced composite material for bone implant," *European Journal of Scientific Research* , vol. 54, pp. 384-406, 2011.
- [37] Semih Benli, Sami Akosy, Hasan Havitcioglu, and Mumin Kucuk, "Evaluation of bone plate with low-stiffness material in terms of stress distribution," *Journal of Biomechanics*, vol. 41, pp. 3229-3235, 2008.

- [38] A. J. Tonino, C. L. Davidson, P. J. Klopper, and L. A. Linclau, "Protection from stress in bone and its effects. Experiments with stainless steel and plastic plates in dogs.," *Journal of Bone and Joint Surgery*, vol. 58, pp. 107-113, 1976.
- [39] K. Tayton and J. Bradley, "How stiff should semi-rigid fixation of human tibia be? A clue to the answer," *The Journal of Bone and Joint Surgery*, vol. 65B, pp. 312-315, 1983.
- [40] S. M. Parren, "Evolution of the internal fixation of long bone fractures," *Journal of Bone Joint Surgery*, vol. 84B, pp. 1093-1100, 2002.
- [41] L. Claes, "The mechanical and morphological properties of bone beneath internal fixation plates of differing rigidity," *Journal of Orthopaedic Research*, vol. 7, pp. 170-177, 1989.
- [42] F.C. Denboer et al., "Quantification of fracture healing with three-dimensional computed tomography," *Archives of Orthopaedic and Trauma Surgery*, vol. 117, pp. 345-350, 1998.
- [43] Hyun-Jun Kim, Suk-Hun Kim, and Seung-Hwan Chang, "Bio-mechanical analysis of a fractured tibia with composite bone plates according to the diaphyseal oblique fracture angle," *Composites: Part B*, vol. 42, pp. 666-674, 2011.
- [44] Suk-Hun Kim, Seung-Hwan Chang, and Dae-Sung Son, "Finite element analysis of the effect of bending stiffness and contact condition of composite bone plates with simple rectangular cross-section on the bio-mechanical behaviour of fractured long bones," *Composites: Part B*, vol. 42, pp. 1731-1738, 2011.

11. Appendix A

In this appendix, photos of some of the tested samples are shown for the purpose of illustrating how they fractured. Figure 57 and 58 show the types of failures resultant from tensile loading. The majority of samples broke in the transverse direction, however, some sample had a combined failure in both the longitudinal and transverse direction combined with partial delamination. In Figure 59 to Figure 62 the types of failures resultant from flexural loads are shown. Some samples simply failed due to tensional failure of the outer surface layers while others had more complex failure patterns including compressive failures of inner surface layers the and delamination.



Figure 57: Failure of samples under tensile load - vertical view



Figure 58: Failure of samples under tensile load - horizontal view



Figure 59: Simple outer-surface failure under flexural load



Figure 60: Simple outer-surface failure under flexural load - close view



Figure 61: Combined outer-surface tensional failure and inner-surface compressive failure under flexural load



Figure 62: Complex outer-surface tensional failure, inner-surface compressive failure, and delamination under flexural load

12. Appendix B

In this appendix, equations that were used in calculations are listed.

Tensile Relations:

$$\text{Tensile stress: } \sigma = \frac{P}{A}$$

$$\text{Young's Modulus: } E = \frac{\sigma}{\varepsilon}$$

Flexural Relations:

$$\text{Maximum flexural stress: } \sigma = \frac{3PL}{2bh^2}$$

$$\text{Maximum strain: } \varepsilon = \frac{6\delta h}{L^2}$$

$$\text{Flexural (secant) Modulus: } E_f^{\text{secant}} = \frac{L^3 m}{4bh^3}$$

Beam Deflection:

$$\text{Maximum deflection: } v_{\text{max}} = \frac{-PL^3}{48EI}$$

$$\text{Area moment of inertia: } I = \frac{1}{12}bh^3$$